Pergamon

Int. J. Solids Structures Vol. 35, No. 22, pp. 2931–2958, 1998

0020–7683/98 $19.00 + .00

PII: S0020–7683(97)00350–8

AN APPROXIMATE ANALYTICAL 3-D SOLUTION FOR THE STRESSES AND STRAINS IN EIGENSTRAINED CUBIC MATERIALS

W. H. MÜLLER* and S. NEUMANN†
Laboratorium für Technische Mechanik, FB 10 Universität-Gesamthochschule-Paderborn, Pohlweg 47-49, 33098 Paderborn, Germany

(*Received* 18 *July* 1997; *in revised form* 27 *October* 1997)

Abstract—A general solution for the total strains that develop in elastically homogeneous and arbitrarily eigenstrained linear-elastic bodies is derived by means of continuous Fourier transforms (CFT). The solution is specialized to the case of a dilatorically eigenstrained spherical region in an infinite body, both of which are made of the same cubic material. It is shown that, for "slight" cubic anisotropy, all integrations can be performed in closed-form. Moreover, the stress–strain fields inside of the inclusion prove to be of the Eshelby type, i.e., they are homogeneous and isotropic. The range of validity of the closed-form solution is investigated numerically by means of discrete Fourier transforms (DFT). It is demonstrated that, even for strongly cubic materials, the closed-form solution is still useful in order to perform parameter studies. Finally, the total elastic energy of two eigenstrained spheres in slightly cubic material is calculated in closed-form by means of CFT. The minimum of this energy is determined as a function of relative position of the two inclusions with respect to the crystal axes and it is used to explain the formation of preferred textures in cubic materials.

1. INTRODUCTION

The presence of inclusions in a solid very frequently leads to the formation of eigenstresses and eigenstrains. Physically speaking, there are two predominant reasons for their occurrence. First, they can be due to a thermal mismatch between the matrix and the inhomogeneity and, second, they can result from a phase transformation, i.e., a spontaneous change of the lattice parameters of the inclusion. Figure 1 shows a dynamic dark-field transmission micrograph of an Alumina crystal containing almost spherical Zirconia inclusions in the tetragonal modification. The presence of thermal eigenstrains becomes visible in form of "contrast fringes" which are located around the mismatched spheres (Mader, 1987). It should be pointed out that the occurrence of these fringes is a three-dimensional effect in the sense that the inclusion represents a spatial defect of finite size. Figure 2 (Dreyer and Olschewski, 1994) illustrates the effects of eigenstresses due to phase transformations in Ni-based single crystal superalloys. The first micrograph shows the initial morphology of cuboidal γ'-precipitates embedded in a γ-matrix in a more or less square-like manner (cf., e.g., Ignat *et al.*, 1993; Socrate and Parks, 1993; Hazotte and Lacase, 1994). Local eigenstresses arise because of the different lattice parameters of the γ/γ'-materials and they eventually lead to a growth of the cubes when the material is aged at elevated temperatures (micrograph (b)). Moreover, if an additional external stress is imposed on the material the cubes will link up and form raft- or plate-like structures as shown in the third and fourth picture.

Fourier transforms are an effective method to handle eigenstrain problems in arbitrarily anisotropic, linear-elastic bodies. The key to the general solution of eigenstress problems is

* Author to whom correspondence should be addressed.
† All names are in alphabetical order.

to map the corresponding system of partial differential equations in physical space onto a system of linear equations in Fourier space which, at least formally, can easily be solved (Mura, 1987). However, in the case of continuous Fourier transforms (CFT), the difficult task is to find the inverse transformation: even for very simple forms of the inclusions it is extremely cumbersome to perform a closed-form integration. This was demonstrated for the two-dimensional case of eigenstrained cylinders in a recent paper by Dreyer *et al.* (1997).

This paper focuses on three-dimensional problems with an emphasis on explicit, closed-form solutions. Specifically, the residual strains in and around a dilatorically eigenstrained sphere in an infinite cubic matrix with the same crystallographic orientation is computed by application of CFT and by specialization to "slight" anisotropy. The accuracy of the closed-form solution is checked by means of discrete Fourier transforms (DFT), a numerical technique which is able to handle any degree of anisotropy. It turns out that even for a higher degree of anisotropy the closed-form solutions is still surprisingly accurate and, consequently, may be used for parameter studies of inclusion problems in typical single crystal materials, such as Alumina or Ni-based superalloys. As a second example of a non-trivial closed-form solution, the elastic energy stored in a body with two dilatorically eigenstrained spheres is computed. As in the case of the strains use will be made of the "slight" anisotropy concept. The energy obtained is a function of the eigenstrains of the two spheres, their diameters, their relative distance and their orientation with respect to the main crystallographic axes. By minimization of the energy it becomes possible to explain the preferred orientation of precipitates in cubic matrices, as reported above.

2. THE GENERAL SOLUTION OF EIGENSTRAIN PROBLEMS IN FOURIER SPACE

Consider an infinite linear-elastic body which contains an eigenstrained region of finite size such that the average of the resulting total strains, ε_{ij}, vanishes. Then the general solution for the total strains in Fourier space, $\hat{\varepsilon}_{ij}$,† can be written as follows (see Mura, 1987, p. 13; or Dreyer *et al.*, 1997):

$$\hat{\varepsilon}_{ij}(\underline{k}) = \hat{A}_{ijkl}(\underline{k})\hat{\varepsilon}^{*}_{kl}(\underline{k}). \tag{2.1}$$

In this equation $\underline{k}$ denotes the (continuous) position vector in (infinite) Fourier space, and $\hat{\varepsilon}^{*}_{kl}$ is the Fourier transform of the eigenstrains which, as it will be shown explicitly in Sections 3 and 5, is a known function of $\underline{k}$ and, among other things, depends upon the shape of the eigenstrained region. The symbols $\hat{A}_{ijkl}$ can be defined in terms of $\underline{k}$ and of the stiffness tensor C_{ijkl}.‡

$$\hat{A}_{ijkl} = \begin{cases} 0, & \text{if } \underline{k} = \underline{0} \\ -\dfrac{1}{2D}(k_i N_{js} + k_j N_{is}) C_{srkl} k_r, & \text{if } \underline{k} \neq \underline{0} \end{cases} \tag{2.2}$$

where N_{ij} and D are the adjunct and the determinant of the following matrix, respectively:

$$M_{ik} = -C_{ijkl}k_j k_l, \quad M^{-1}_{ij} = \frac{N_{ij}}{D}, \quad D = \det \underline{\underline{M}}. \tag{2.3}$$

Specifically, a cubic material is characterized by three elastic constants and its stiffness tensor is given by:

$$\begin{aligned} C_{ijkl} &= \lambda\delta_{ij}\delta_{kl} + \mu(\delta_{ik}\delta_{jl} + \delta_{il}\delta_{jk}) + \mu'\delta_{ijkl} \\ &= C_{12}\delta_{ij}\delta_{kl} + C_{44}(\delta_{ik}\delta_{jl} + \delta_{il}\delta_{jk}) + (C_{11} - C_{12} - 2C_{44})\delta_{ijkl} \end{aligned} \tag{2.4}$$

† In this paper Fourier transformed quantities are identified by a hat.

‡ In what follows the notation of this paper differs by a minus from the one used by Mura (1987).

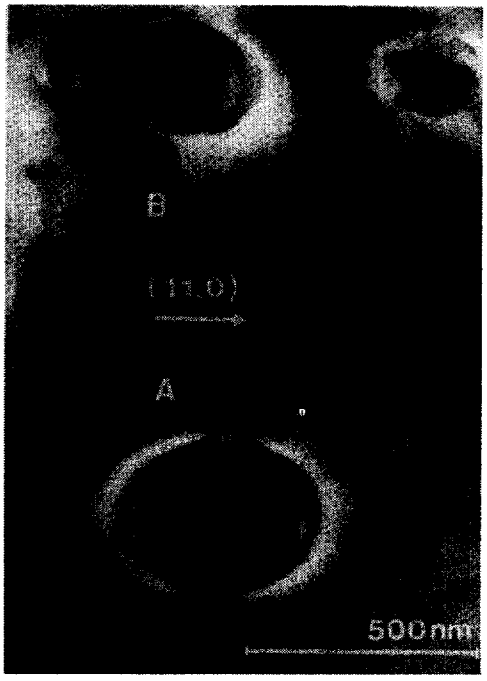

Fig. 1. Thermal contrast fringes around spherical Zirconia inclusions in Alumina matrix (Mader, 1987).

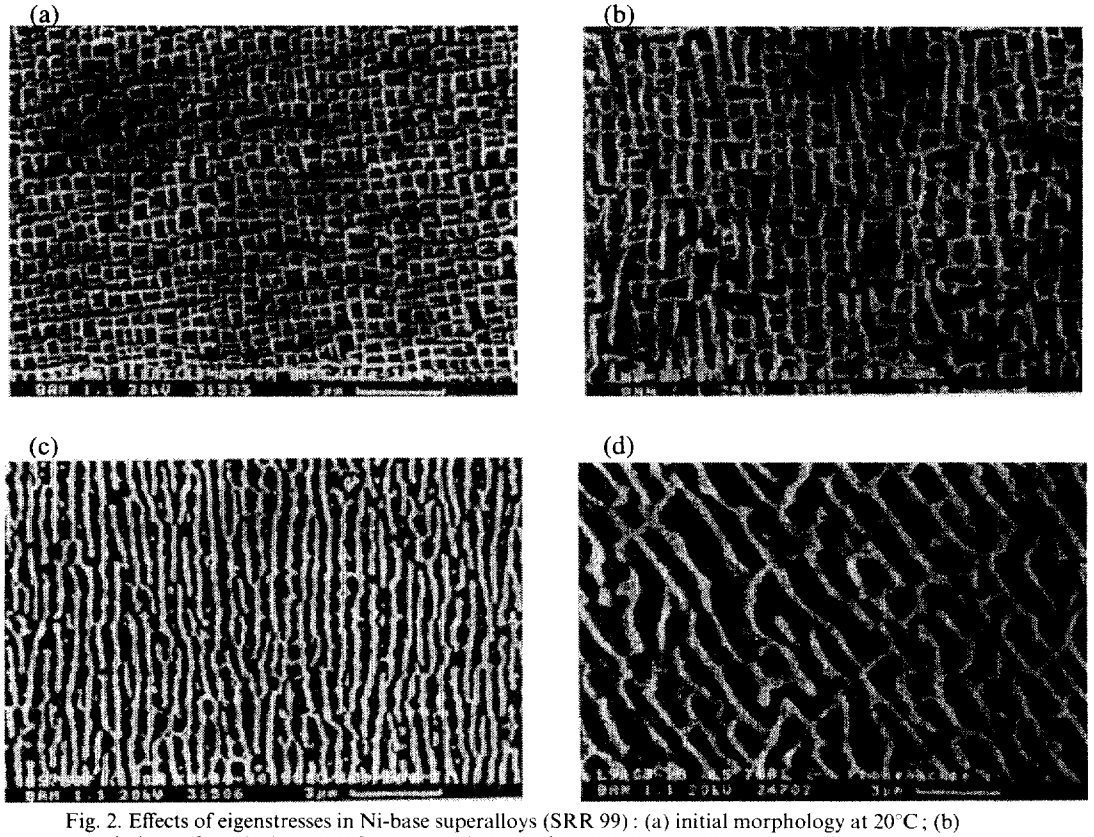

Fig. 2. Effects of eigenstresses in Ni-base superalloys (SRR 99): (a) initial morphology at 20°C; (b) morphology after 500 h at 980°C; (c) morphology after 50 h in a tensile creep test (load axes→); (d) morphology after 230 h in a cyclic test (load axes↔) (Dreyer and Olschewski, 1994).

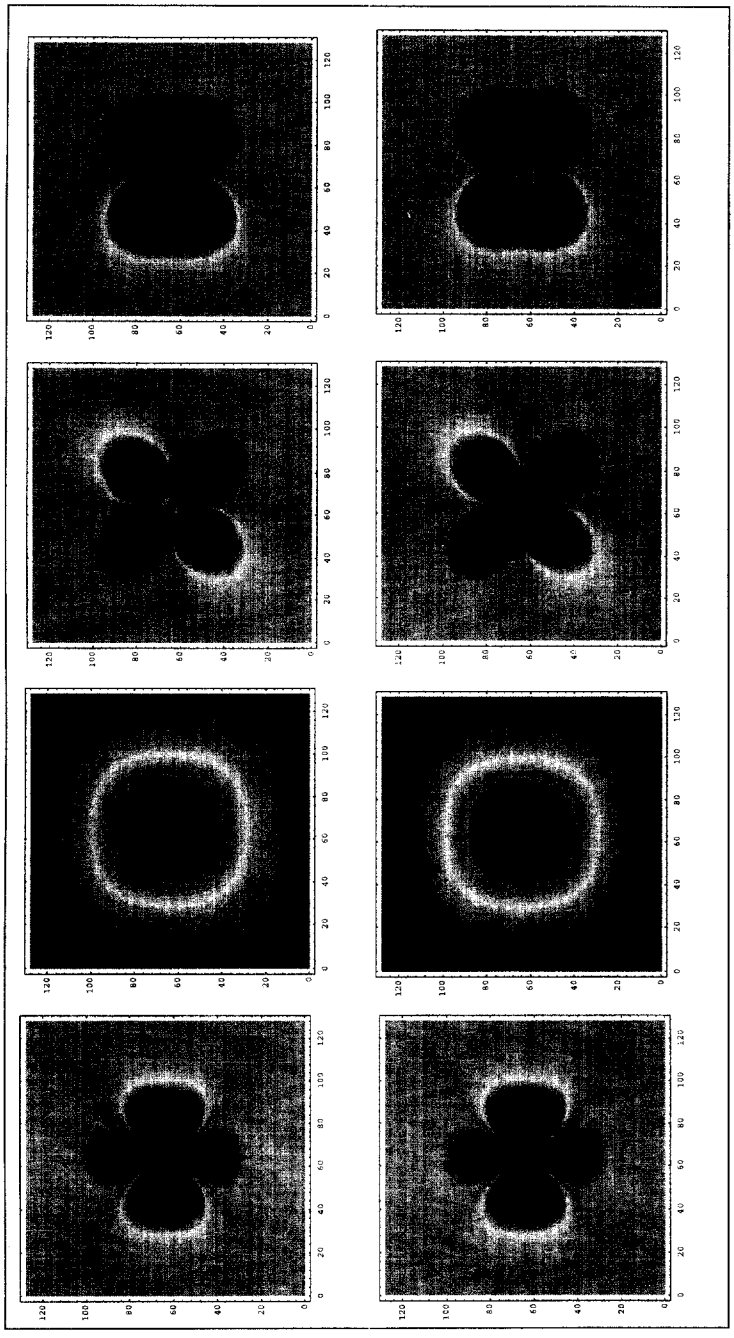

Fig. 4a. Total strains ε_{11}, ε_{33}, ε_{12}, and ε_{23} in the median plane of a spherical inclusion in an aluminum single crystal; pictures on the top were computed by DFT, pictures on the bottom follow from the closed-form solution.

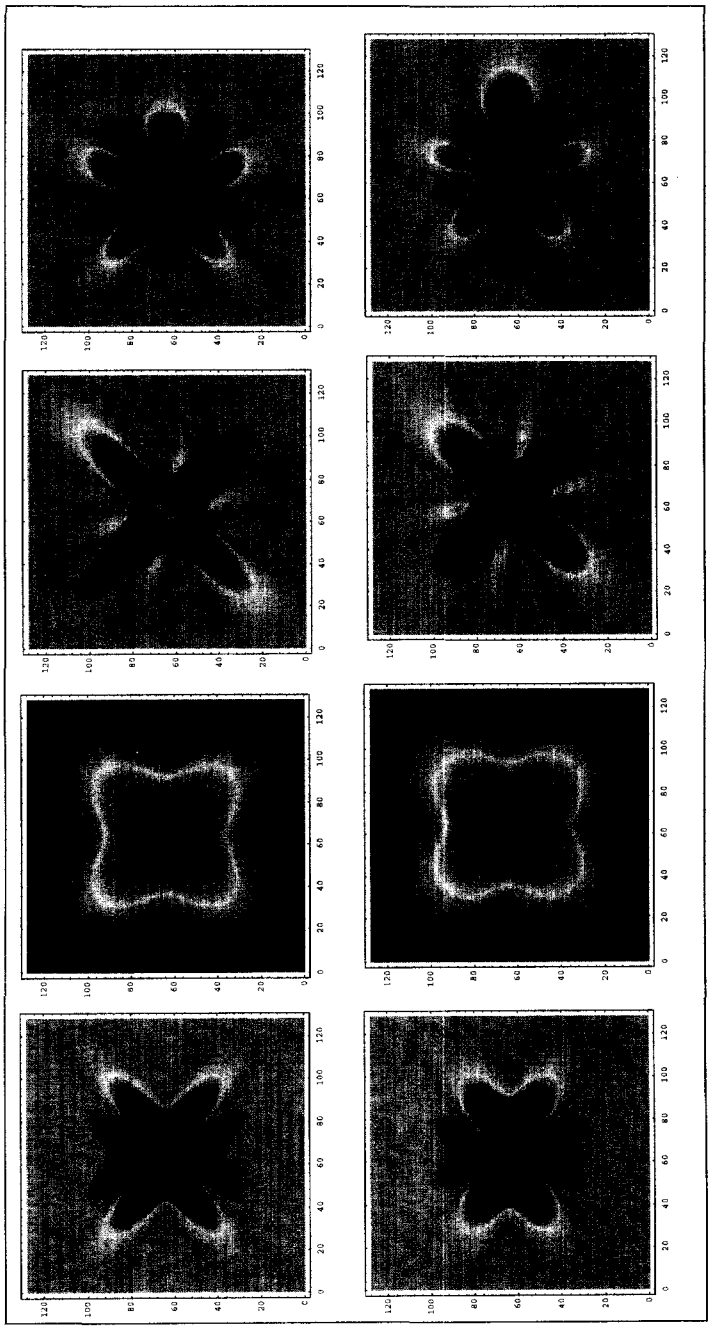

Fig. 4b. Total strains ε_{11}, ε_{33}, ε_{12}, and ε_{23} in the median plane of a spherical inclusion in a silver single crystal; pictures on the top were computed by DFT, pictures on the bottom follow from the closed-form solution.

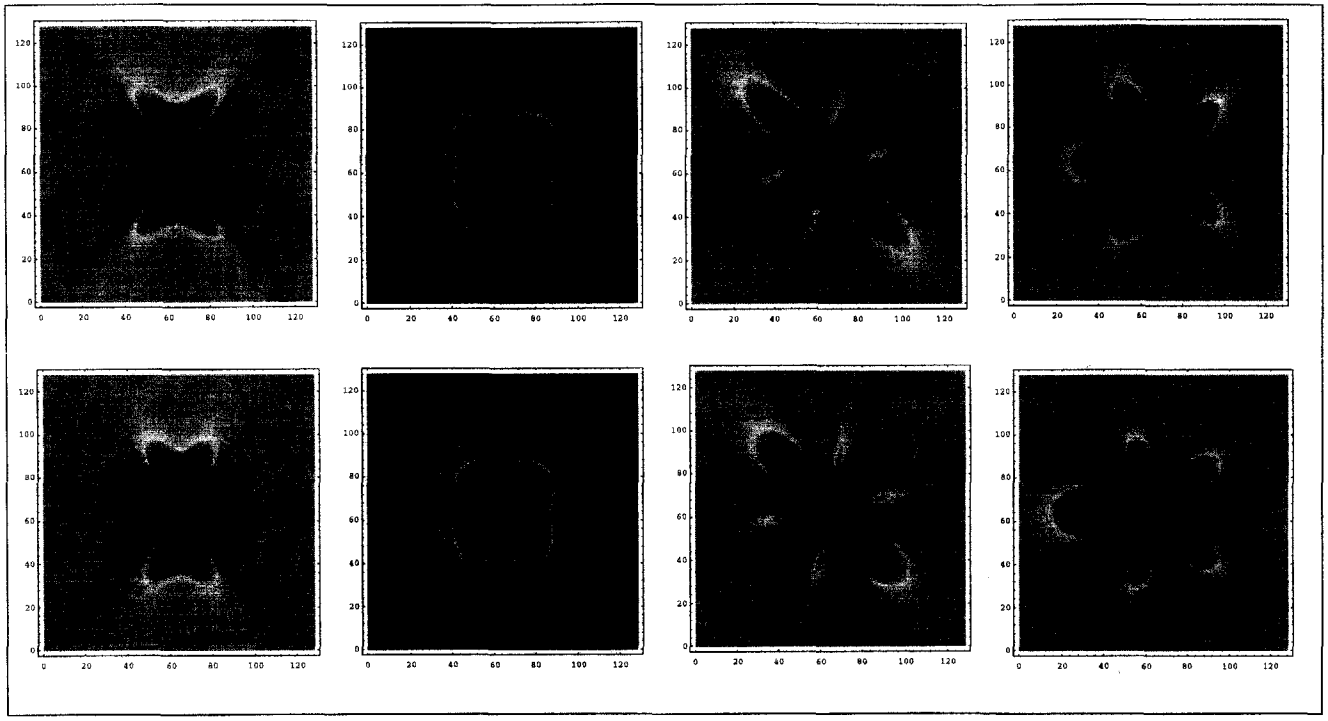

Fig. 4c. Total strains ε_{11}, ε_{33}, ε_{12}, and ε_{23} in the median plane of a spherical inclusion in a Ni-based single crystal superalloy; pictures on the top were computed by DFT, pictures on the bottom follow from the closed-form solution.

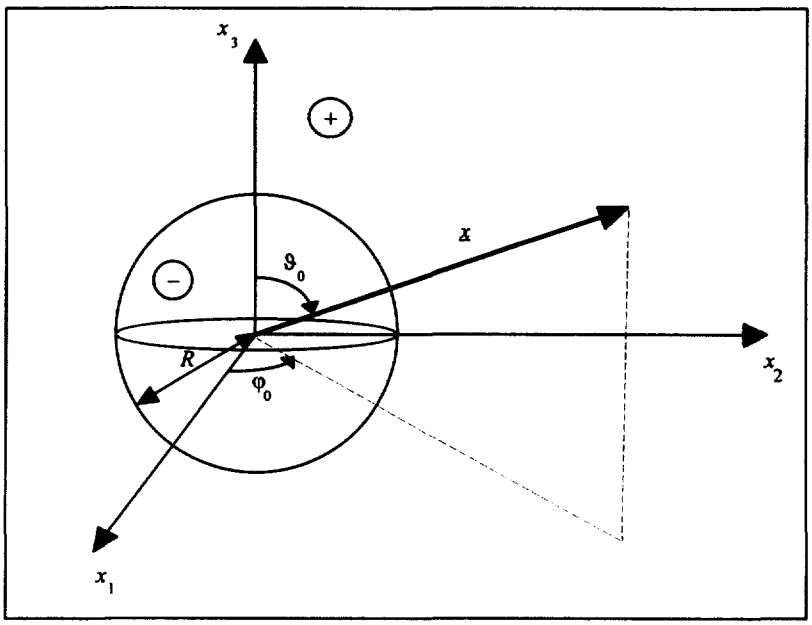

Fig. 3. An eigenstrained sphere in a cubic matrix.

where δ_{ij} and δ_{ijkl} denote two- and four-dimensional Kronecker symbols. Moreover, λ, μ, μ' are Lamé's constants and the anisotropy coefficient, respectively, and the symbols C_{ij} denote Voigt's constants. By means of this equation it follows that in three-dimensional space (Mura, 1987, p. 14):

$$N_{11}(\underline{k}) = -(\mu^2 k^4 + \beta k^2 (k_2^2 + k_3^2) + \gamma k_2^2 k_3^2), \tag{2.5}$$

$$N_{12}(\underline{k}) = (\lambda+\mu) k_1 k_2 (\mu k^2 + \mu' k_3^2), \ldots \tag{2.6}$$

$$D = \mu^2 (\lambda+2\mu+\mu') k^6 + \mu\mu' (2\lambda+2\mu+\mu') k^2 k_\Sigma + \mu'^2 (3\lambda+3\mu+\mu') k_\Pi \tag{2.7}$$

where the following contractions have been used:

$$k = \sqrt{k_1^2+k_2^2+k_3^2}, \quad k_\Sigma = k_1^2 k_2^2 + k_1^2 k_3^2 + k_2^2 k_3^2, \quad k_\Pi = k_1^2 k_2^2 k_3^2, \tag{2.8}$$

$$\beta = \mu(\lambda+\mu+\mu'), \quad \gamma = \mu'(2\lambda+2\mu+\mu'). \tag{2.9}$$

All other components of N_{ij} can be obtained from the cited ones by a consistent change of indices.

In principle, the total strains in physical space can be obtained from eqn (2.1) by inverse Fourier transform (see Dreyer *et al.*, 1997, for the conventions used) as follows:

$$\varepsilon_{ij}(\underline{x}) = \frac{1}{(2\pi)^{3/2}} \int_{-\infty}^{+\infty} \hat{A}_{ijkl} \hat{\varepsilon}_{kl}^{*} \exp(-i\underline{k} \cdot \underline{x}) \, \mathrm{d}\underline{k}. \tag{2.10}$$

However, even for a simple spherical geometry of the eigenstrained region the integrations involved are by no means trivial.

3. A SPHERE IN A CUBIC MATRIX

Consider the situation shown in Fig. 3: a dilatorically eigenstressed sphere, "−", of radius R is inserted in a cubic matrix, "+", made of the same cubic material with the same orientation of the crystal axes. Consequently, the eigenstrains are given by:

Table 1. On the smallness of the parameter Λ (based on data from Auld, 1990, and Socrate and Parks, 1993)

Material (cubic single crystal)	μ^*	$\Lambda_{max} \leqslant (\lvert B_1\mu^*\rvert/3)+(\lvert B_2\mu^{*2}\rvert/27)$
Aluminum	−0.36	0.2
Iron	−1.17	0.76
Nickel	−1.24	0.83
Silver	−1.32	0.96
Gold	−1.31	0.99
Nickel-based superalloy†	−1.33	0.93

† Data after Pollock and Argon from the paper by Socrate and Parks, 1993; the arithmetic averages of the elastic constants of the γ/γ' phases are shown.

$$\varepsilon_{ij}^*(\underline{x}) = \varepsilon_0\theta(\underline{x})\delta_{ij}, \quad \theta(\underline{x}) = \begin{cases} 1, & \forall \underline{x} \text{ in } - \\ 0, & \forall \underline{x} \text{ in } + \end{cases}, \tag{3.1}$$

and ε_0 is a constant which characterizes the intensity of the eigenstrain. If this equation is used together with eqns (2.2) and (2.5–2.9) the following result for the strains in Fourier space is obtained:

$$\hat{\varepsilon}_{ij}(\underline{k}) = B\varepsilon_0 \frac{\Gamma_{ij}(\underline{k})}{1+\Lambda(\underline{k})}\hat{\theta}(\underline{k}), \tag{3.2}$$

where

$$\Lambda(\underline{k}) = B_1\frac{k_\Sigma}{k^4}\mu^* + B_2\frac{k_\Pi}{k^6}(\mu^*)^2, \tag{3.3}$$

$$\Gamma_{11}(\underline{k}) = (1+\mu^*)\frac{k_1^2}{k^2} - \mu^*\frac{k_1^4}{k^4} + (\mu^*)^2\frac{k_\Pi}{k^6}, \tag{3.4}$$

$$\Gamma_{12}(\underline{k}) = \left(1+\frac{\mu^*}{2}\right)\frac{k_1k_2}{k^2} + \mu^*(1+\mu^*)\left(\frac{k_1k_2k_3^2}{2k^4}\right) - (\mu^*)^2\frac{k_1k_2k_3^4}{2k^6}, \tag{3.5}$$

$$B = \frac{3\lambda+2\mu+\mu'}{\lambda+2\mu+\mu'}, \quad B_1 = \frac{2\lambda+2\mu+\mu'}{\lambda+2\mu+\mu'}, \quad B_2 = \frac{3\lambda+3\mu+\mu'}{\lambda+2\mu+\mu'}, \quad \mu^* = \frac{\mu'}{\mu}, \tag{3.6}$$

and all the other components of Γ_{ij} can be obtained by index substitution.

The integration in Fourier space can be performed in closed-form if the denominator in eqn (3.2) is expanded with respect to the parameter Λ. A similar procedure has been used before to simplify expressions when computing elastic energies in Fourier space (see, e.g., McCormack *et al.*, 1992; Wang *et al.*, 1992; Dreyer *et al.*, 1997). Furthermore, note that:

$$\frac{k_\Sigma}{k^4} \leqslant \frac{1}{3}, \quad \frac{k_\Pi}{k^6} \leqslant \frac{1}{27}. \tag{3.7}$$

Table 1 presents elastic data for various cubic single crystals together with the computed values for the maximum of the parameter Λ. It must be concluded that Λ is by no means $\ll 1$ for most materials. However, it will be demonstrated by comparison with numerical results obtained from DFT that, from a practical point of view, it is sufficient to take only

a first order term with respect to Λ into account and to neglect quadratic terms in μ^*.† Physically speaking, this may be interpreted as a slight deviation from the case of isotropic materials:

$$\hat{\varepsilon}_{ij} \approx B\varepsilon_0 U_{ij}\hat{\theta} \tag{3.8}$$

where:

$$U_{11}(\underline{k}) = (1+\mu^*)\frac{k_1^2}{k^2} - \mu^*\left(\frac{k_1^4}{k^4} + B_1\frac{k_1^2}{k^2}\frac{k_\Sigma}{k^4}\right), \tag{3.9}$$

$$U_{12}(\underline{k}) = \left(1+\frac{\mu^*}{2}\right)\frac{k_1 k_2}{k^2} + \frac{\mu^*}{2}\left(\frac{k_1 k_2 k_3^2}{k^4} - 2B_1\frac{k_1 k_2}{k^2}\frac{k_\Sigma}{k^4}\right), \ldots, \tag{3.10}$$

and all the other components of U_{ij} can be obtained by index substitution.

After insertion of these results into eqn (2.10) and integration with respect to $\underline{k}$ the following strain fields are obtained for the inside of the sphere:

$$\bar{\varepsilon}_{ij} \approx \varepsilon_0\frac{B}{3}\begin{bmatrix} \underline{1}+\dfrac{\mu^*}{5}(2-B_1) & 0 & 0 \\ 0 & \underline{1}+\dfrac{\mu^*}{5}(2-B_1) & 0 \\ 0 & 0 & \underline{1}+\dfrac{\mu^*}{5}(2-B_1) \end{bmatrix} \tag{3.11}$$

and for the outside of the cylinder:

$$\begin{aligned}
\bar{\varepsilon}_{11} \approx B\varepsilon_0\frac{R^3}{r^3}\Bigg\{&\left[\frac{1}{3} - \left(\frac{1}{6}-\frac{5}{24}B_1\right)\mu^* + \left(\frac{3}{10}-\frac{13}{20}B_1\right)\mu^*\frac{R^2}{r^2} + \frac{3}{8}B_1\mu^*\frac{R^4}{r^4}\right] \\
&+\left[-\underline{1}+\left(2-\frac{13}{4}B_1\right)\mu^* + (-3+10B_1)\mu^*\frac{R^2}{r^2} - \frac{27}{4}B_1\mu^*\frac{R^4}{r^4}\right]\frac{x_1^2}{r^2} \\
&+\left[\frac{5}{2}(-1+3B_1)\mu^* + \frac{7}{2}(1-7B_1)\mu^*\frac{R^2}{r^2} + 18B_1\mu^*\frac{R^4}{r^4}\right]\frac{x_1^4}{r^4} \\
&+\frac{B_1}{8}\mu^*\left[-5+14\frac{R^2}{r^2} - 9\frac{R^4}{r^4}\right]\frac{x_2^2 x_3^2}{r^4} \\
&+\frac{B_1}{8}\mu^*\left[-35+126\frac{R^2}{r^2} - 99\frac{R^4}{r^4}\right]\left[\frac{x_1^6}{r^6} - \frac{x_1^2 x_2^2 x_3^2}{r^6}\right]\Bigg\},
\end{aligned} \tag{3.12}$$

$$\begin{aligned}
\bar{\varepsilon}_{12} \approx B\varepsilon_0\frac{R^3}{r^3}\Bigg\{&\left[-\underline{1}+\left(\frac{1}{2}-\frac{15}{8}B_1\right)\mu^* + \left(-\frac{3}{2}+\frac{27}{4}B_1\right)\mu^*\frac{R^2}{r^2} - \frac{39}{8}B_1\mu^*\frac{R^4}{r^4}\right]\frac{x_1 x_2}{r^2} \\
&+\mu^*\left[\frac{5}{8}(-2+9B_1) + \frac{1}{8}(14-154B_1)\frac{R^2}{r^2} + \frac{117}{8}B_1\frac{R^4}{r^4}\right]\left[\frac{x_1^3 x_2 + x_1 x_2^3}{r^4}\right]
\end{aligned}$$

†The same concept has been used before in Dreyer *et al.* (1997) to treat the two-dimensional case of an eigenstrained cylinder. It is interesting to note that if the denominator in eqn (3.2) is considered as a function of μ^* and expanded with respect to this parameter (including an expansion of the constants B, B_1, and B_2) the comparison of the resulting first order approximation with the numerical data is not as favorable as the comparison with the result presented above.

$$+\frac{B_1\mu^*}{8}\left[-35+126\frac{R^2}{r^2}-99\frac{R^4}{r^4}\right]\left[\frac{x_1^5x_2+x_1x_2^5+x_1^3x_2^3}{r^6}\right]\Bigg\},\ldots. \quad (3.13)$$

In these equations $r = |\underline{x}|$ denotes the radial distance from the origin. As before the other components can be obtained by suitable index substitution.

Note that this solution is of the Eshelby-type, i.e., the fields are homogeneous and isotropic within the sphere. The proof of these equations is presented in Appendix A. The usefulness of this approximate solution, even for strongly anisotropic materials, such as silver, or Ni-based superalloys will be demonstrated in the next section by comparing it with results from DFT applied to the problem of an eigenstrained sphere in a cubic matrix. Note that the underlined terms in eqns (3.12) and (3.13) are identical to Lamé's solution when specialized to the case of a spherical misfit which is inserted into an infinite matrix made of isotropic material. In this case the constant B reduces to:

$$B = \frac{1+\nu}{1-\nu}. \quad (3.14)$$

This solution is normally written in polar coordinates. In Cartesian coordinates, x_i, it reads:

$$\varepsilon_{ij}(\underline{x}) = \frac{\varepsilon_0(1+\nu)}{3(1-\nu)} \times \begin{cases} \delta_{ij}, & \text{in } - \\ \dfrac{R^3}{r^3}\left(\delta_{ij}-3\dfrac{x_ix_j}{r^2}\right), & \text{in } + \end{cases}. \quad (3.15)$$

4. COMPARISON WITH DISCRETE FOURIER TRANSFORMS

The objective of this section is to test the range of validity of the analytical results for the strains in and around an eigenstrained sphere in a cubic matrix shown in eqns (3.11)–(3.13). It is worth mentioning that these expressions are based on an approximation and, physically speaking, should be interpreted as a slight deviation from the isotropic case. DFT was used to calculate the strains numerically for three different materials, namely for aluminum:

$$\lambda = 61{,}300 \text{ MPa}, \quad \mu = 28{,}500 \text{ MPa}, \quad \mu' = -10{,}300 \text{ MPa}, \quad \varepsilon_0 = 0.005 \quad (4.1)$$

for silver:

$$\lambda = 89{,}400 \text{ MPa}, \quad \mu = 43{,}700 \text{ MPa}, \quad \mu' = -57{,}800 \text{ MPa}, \quad \varepsilon_0 = 0.005, \quad (4.2)$$

and for the Ni-based superalloy of Table 1:

$$\lambda = 12{,}500 \text{ MPa}, \quad \mu = 91{,}500 \text{ MPa}, \quad \mu' = -122{,}000 \text{ MPa}, \quad \varepsilon_0 = -0.0039. \quad (4.3)$$

The number of discretization points per dimension was chosen to be:

$$N = 128. \quad (4.4)$$

All calculations were performed on a SPARC-Server 1000 and the plots were generated by means of routines from Mathematica® (Wolfram, 1992).

Note that a special discrete Green's operator where spatial derivatives were approximated by difference quotients was used during the DFT analysis. Some details can be found in the work of Dreyer (1995) and in the paper by Müller (1996). An alternative discretization

procedure based on the continuous Green's operator was used in the work of Moulinec and Suquet (1994, 1996, 1997).

The density plots shown in Fig. 4 allow one to gain an overview of the stress components ε_{11}, ε_{33}, ε_{12} and ε_{23} in the plane $(x_1, x_2, x_3 = 0)$ for all three materials considered. The plots in the top row result from DFT analysis and the plots in the bottom row follow by evaluation of the closed-form solution.

The influence of anisotropy is clearly visible: at $\pm 45°$ the strain gradients of highly cubic materials (silver and Ni-based superalloys) are much more pronounced than in the less anisotropic case (aluminum). Moreover, note that in these more or less qualitative pictures only little differences between the numerical and the analytical results are discernible.

Figure 5 allows one to see these differences in more detail. The sequences present vertical and horizontal cuts through the numerically computed strain fields ε_{11} and ε_{33} together with the corresponding data from the analytical solution of eqns (3.11)–(3.13). In the case of aluminum the agreement is excellent whereas for silver and the Ni-based superalloy the differences become more pronounced. Obviously outside of the sphere the agreement is better than inside. It is interesting to note that this behavior is exactly opposite to the two-dimensional case discussed by Dreyer *et al.* (1997). Moreover, note that the closed-form solution tends to underestimate the maximum of the strains.

5. APPLICATIONS TO THE FORMATION OF TEXTURES

Consider the situation shown in Fig. 6 which shows two spheres of different radii, ρ_1 and ρ_2, embedded in an infinite matrix. The spheres and the matrix are made of the same cubic material with the same orientation of the main crystallographic axes. The eigenstrains, ε^*_{1ij} and ε^*_{2ij}, in the two cylinders are assumed to be purely dilatoric, homogeneous but different:

$$\varepsilon^*_{ij}(\underline{x}) = [\theta_1(\underline{x})\varepsilon^*_1 + \theta_2(\underline{x}-\underline{R})\varepsilon^*_2]\delta_{ij}, \tag{5.1}$$

with shape functions, $\theta_1(\underline{x})$ and $\theta_2(\underline{x})$:

$$\theta_1(\underline{x}) = \begin{cases} 1, & \text{if } |\underline{x}| < \rho_1 \\ 0, & \text{if } |\underline{x}| > \rho_1 \end{cases}, \quad \theta_2(\underline{x}-\underline{R}) = \begin{cases} 1, & \text{if } |\underline{x}-\underline{R}| < \rho_2 \\ 0, & \text{if } |\underline{x}-\underline{R}| > \rho_2 \end{cases}. \tag{5.2}$$

and constants ε^*_1 and ε^*_2.

The objective is to compute the elastic energy stored in this system and to identify the positions, $R_{\min}$, $\varphi_{\min}$, and $\vartheta_{\min}$, of the two spheres for which this energy assumes a minimum. These positions can be used to explain preferred locations for precipitation in cubic materials which eventually leads to the formation of characteristic textures (see Section 1). In fact, energetic arguments have been used before for this purpose: Tien and Copley (1970) or Pineau (1995). For vanishing external loads (n_j being the normal unit vector):

$$f_i^{\partial V} = \sigma_{ij} n_j = 0 \quad \text{on } \partial V, \tag{5.3}$$

the elastic energy can be computed from:

$$\Psi_{\text{el}} = \frac{1}{2}\int_V \sigma_{ij}(\varepsilon_{ij} - \varepsilon^*_{ij})\,\mathrm{d}V = -\frac{1}{2}\int_V \sigma_{ij}\varepsilon^*_{ij}\,\mathrm{d}V \tag{5.4}$$

as is easily seen by application of the kinematic relations:

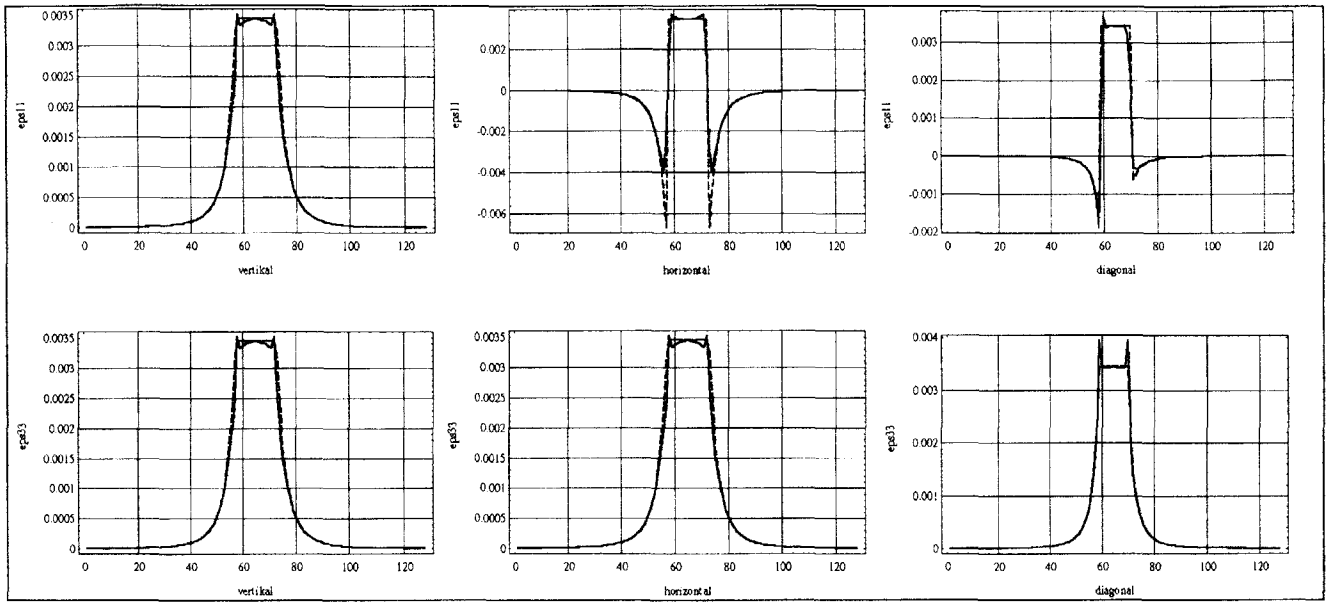

Fig. 5a. Vertical/horizontal/and diagonal cuts through strain fields ε_{11} (top) and ε_{33} (bottom) in the median plane of a spherical inclusion in an aluminum single crystal; full lines correspond to the computation by DFT, dashed lines relate to the closed-form solution.

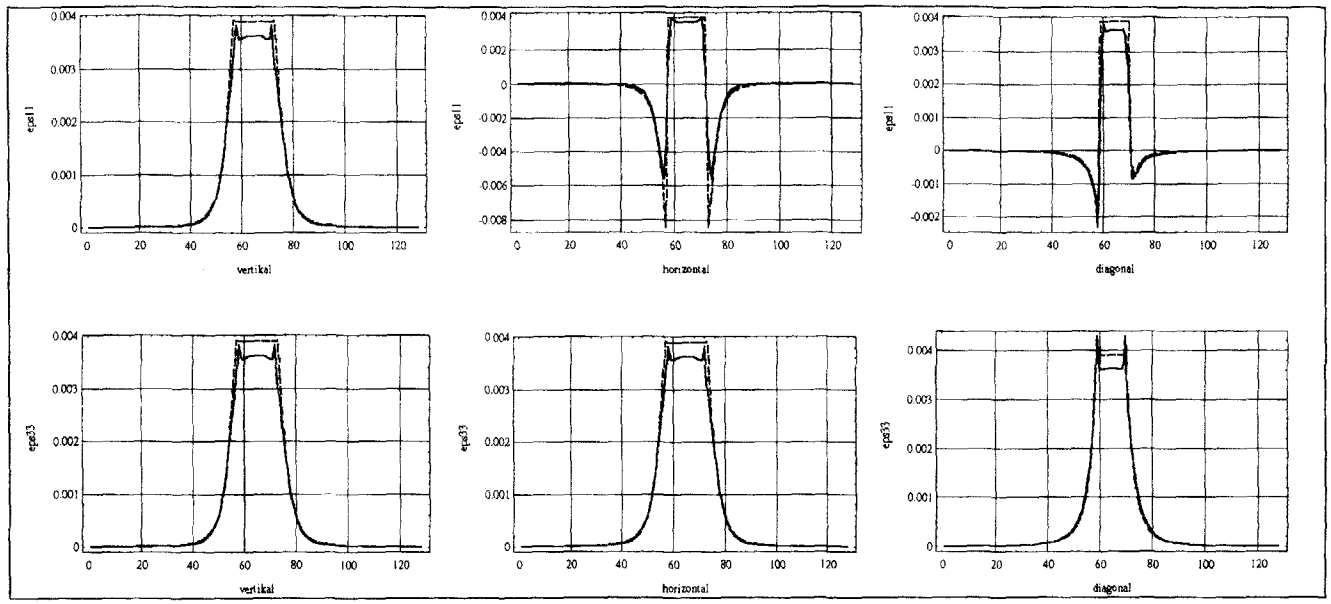

Fig. 5b. Vertical/horizontal/and diagonal cuts through strain fields ε_{11} (top) and ε_{33} (bottom) in the median plane of a spherical inclusion in a silver single crystal; full lines correspond to the computation by DFT, dashed lines relate to the closed-form solution.

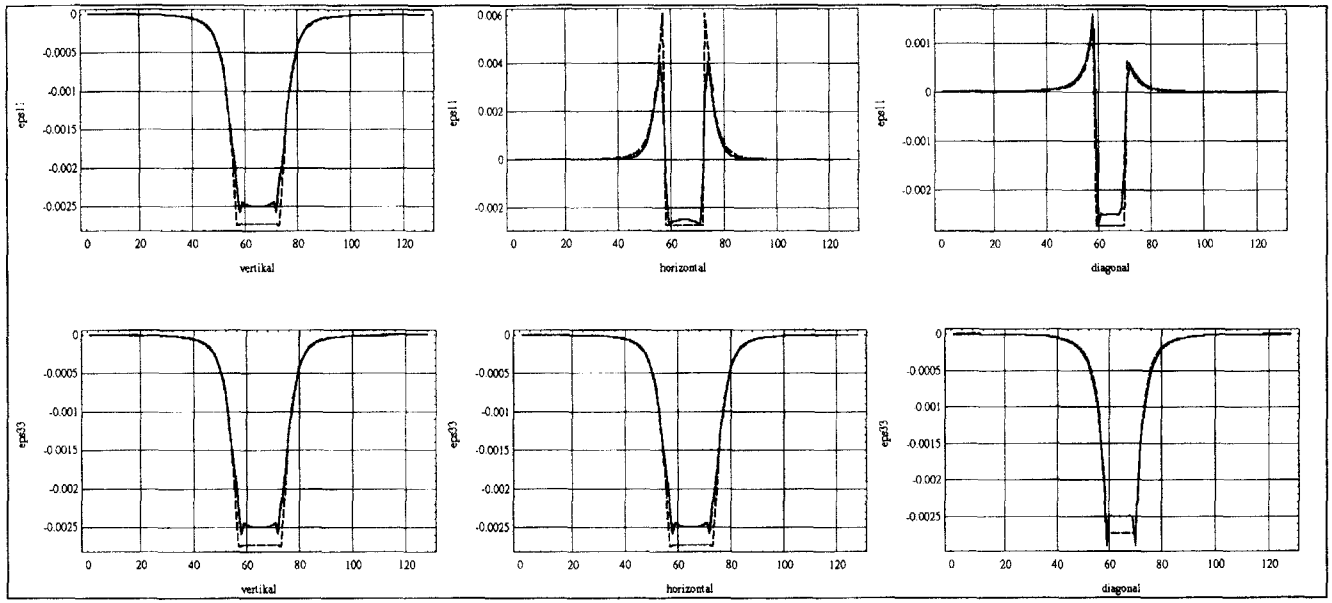

Fig. 5c. Vertical/horizontal/and diagonal cuts through strain fields ε_{11} (top) and ε_{33} (bottom) in the median plane of a spherical inclusion in a Ni-based single crystal superalloy; full lines correspond to the computation by DFT, dashed lines relate to the closed-form solution.

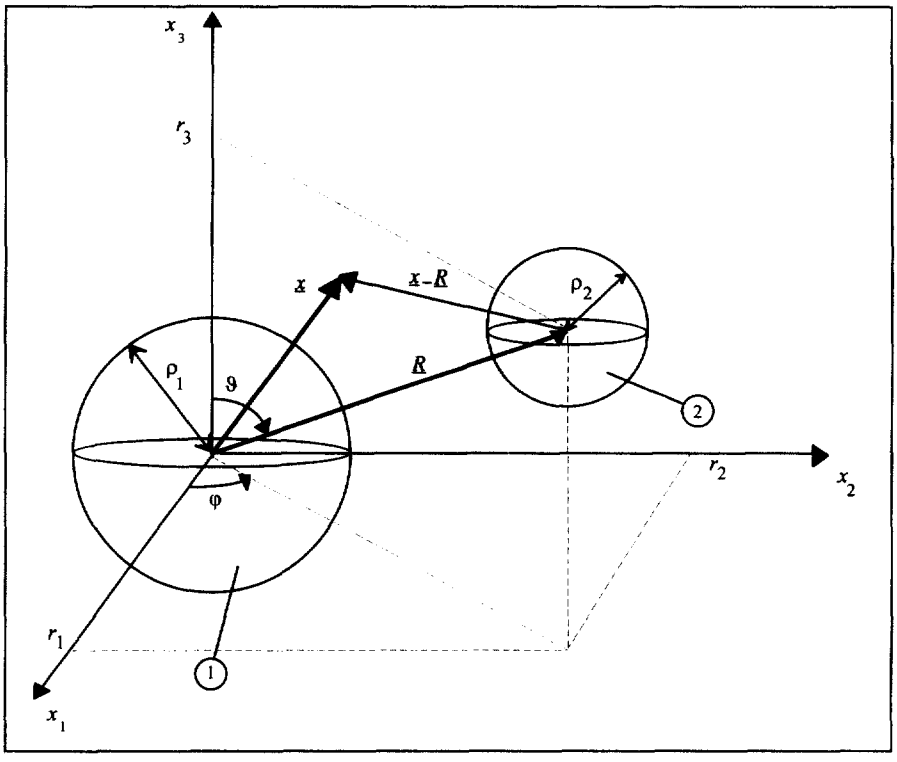

Fig. 6. Two eigenstrained spheres in a cubic matrix.

$$\varepsilon_{ij} = \frac{1}{2}\left(\frac{\partial u_i}{\partial x_j} + \frac{\partial u_j}{\partial x_i}\right), \tag{5.5}$$

Gauss' theorem and the equilibrium of forces:

$$\frac{\partial \sigma_{ij}}{\partial x_j} = 0. \tag{5.6}$$

The position and orientation of the two spheres can be described in standard spherical coordinates, i.e., by a radial distance, R, an azimuthal angle, φ, and a polar angle, ϑ (see Fig. 6).

By virtue of Hooke's law:

$$\sigma_{ij} = C_{ijkl}(\varepsilon_{kl} - \varepsilon^*_{kl}), \tag{5.7}$$

and following the ideas in the work of Khachaturyan and Shatalov (1969) the elastic energy (5.4) can be evaluated in Fourier space by virtue of the power theorem (bars denote complex conjugates):

$$\int_{-\infty}^{+\infty} f(\underline{x})\overline{g(\underline{x})}\,\mathrm{d}\underline{x} = \int_{-\infty}^{+\infty} \hat{f}(\underline{k})\overline{\hat{g}(\underline{k})}\,\mathrm{d}\underline{k} \tag{5.8}$$

to become:

$$\Psi_{el} = \frac{1}{2} C_{ijkl} \int_{\underline{k}} (\hat{\varepsilon}^*_{ij} \overline{\hat{\varepsilon}^*_{kl}} - \hat{A}_{klrs} \hat{\varepsilon}^*_{rs} \overline{\hat{\varepsilon}^*_{ij}}) \, \mathrm{d}\underline{k} \tag{5.9}$$

where the symbol $\hat{A}_{klrs}$ has been explained before in eqn (2.2).

If this expression is evaluated for 3-D problems in cubic materials and for purely dilatoric eigenstrains the following equation results:

$$\Psi_{el} = \tilde{B} \int_{\mathbb{R}^3} (3 - \hat{A}_{llmm}) \hat{\varepsilon}^* \overline{\hat{\varepsilon}^*} \, \mathrm{d}\underline{k} \tag{5.10}$$

where [cp., eqns (2.2), (2.5)–(2.8) and (3.6)]:

$$\hat{A}_{llmm} = B \frac{1 + 2\frac{k_\Sigma}{k^4}\mu^* + 3\frac{k_\Pi}{k^6}(\mu^*)^2}{1 + \Lambda(\underline{k})} \tag{5.11}$$

and:

$$\tilde{B} = \frac{3\lambda + 2\mu + \mu'}{2}. \tag{5.12}$$

In order to enable a closed-form integration a similar procedure is used as in the case of the eigenstrained sphere in cubic material, Section 3: the integrand is expanded with respect to the parameter $\Lambda(\underline{k})$ and only linear terms in μ^* are taken into account. This results in the following closed-form expression for the elastic energy of two eigenstrained spheres in an infinitely large matrix:

$$\psi(R, \varphi, \vartheta) = \frac{\Psi_{el} - \Psi_0}{B_\Psi} = \frac{\rho_1^3 \rho_2^3}{R^3} \left(-5 + 7\frac{\rho_1^2 + \rho_2^2}{R^2} \right) \left(-1 + 5\frac{R_1^2 R_2^2 + R_1^2 R_3^2 + R_2^2 R_3^2}{R^4} \right) \tag{5.13}$$

where a constant, Ψ_0, has been defined as follows:

$$\Psi_0 = \frac{4\pi}{3} \tilde{B} B_3 \left(2 - \frac{1}{5} B\mu^* \right) (\varepsilon_1^{*2} \rho_1^3 + \varepsilon_2^{*2} \rho_2^3), \tag{5.14}$$

and:

$$B_\Psi = \frac{4\pi}{15} \tilde{B} B B_3 \mu^* \varepsilon_1^* \varepsilon_2^*, \quad B_3 = \frac{2\mu + \mu'}{\lambda + 2\mu + \mu'}. \tag{5.15}$$

Note that the angular dependence is hidden in the components (R_1, R_2, R_3) of the distance vector. Details of the integration can be found in Appendix B.

As indicated in Table 1 the parameter μ^* seems to be negative for many metals and, because of its required smallness, it seems reasonable to assume that Ψ_0 and B_Ψ are positive and negative, respectively. Consequently, the fact whether the elastic energy, Ψ_{el}, assumes a local maximum or minimum is determined from the sign of the product $\varepsilon_1^* \varepsilon_2^*$ in combination with the behavior of ψ with respect to (R, φ, ϑ). Table 2 allows one to identify the nature and the location of all extremes of ψ in the first octant where $R_\xi = \sqrt{\frac{7}{3}(\rho_1^2 + \rho_2^2)}$.

Figure 7(a) presents an overall view of $\psi(R_1, R_2, R_3 = 0)$ for the choice $\rho_1 = 1$, $\rho_2 = \frac{1}{5}$. Two characteristic features are clearly visible: the function assumes minima at $\varphi = \pi/4$ with a periodicity of $\pi/2$ and the maxima at $\varphi = 0$ also with a periodicity of $\pi/2$. Note that

Table 2. On the location of the extremes of the energy $\psi(R_1, R_2, R_3)$

Sign of $\varepsilon_1^*/\varepsilon_2^*$	$(R_\xi, 0, \pi/2)$	$(R_\xi, \pi/4, \arccos 1/\sqrt{3})$†	$(R_\xi, 0, 0)$	$(R_\xi, \pi/2, \pi/2)$
+/+ or −/−	Maximum	Minimum	Maximum	Maximum
+/− or −/+	Minimum	Maximum	Minimum	Minimum

† This location corresponds to a position on the spatial diagonal.

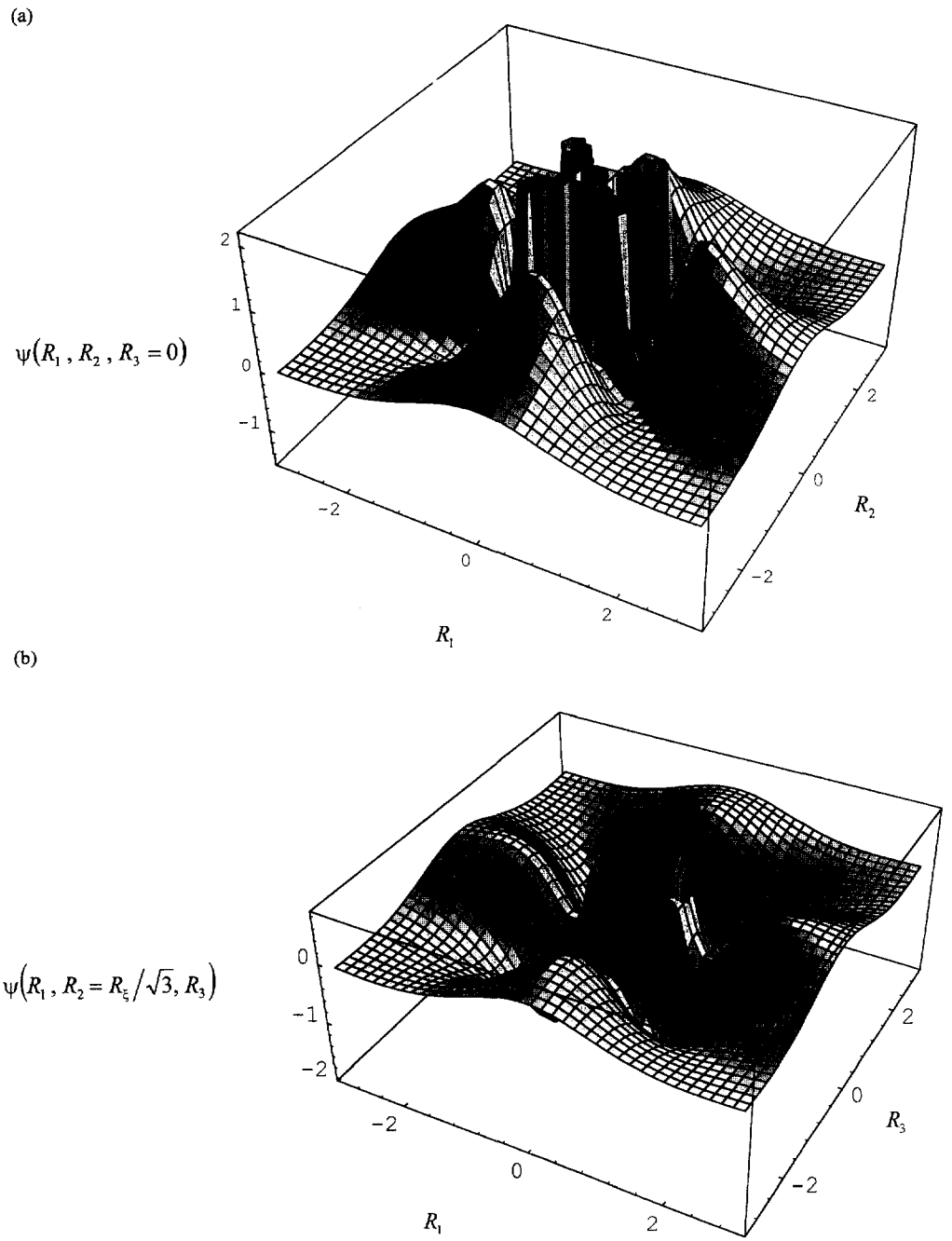

Fig. 7. On the location of the extremes of the energy $\psi(R_1, R_2, R_3)$: (a) the situation $\psi(R_1, R_2, R_3 = 0)$; (b) the situation $\psi(R_1, R_2 = R_\xi/\sqrt{3}, R_3)$.

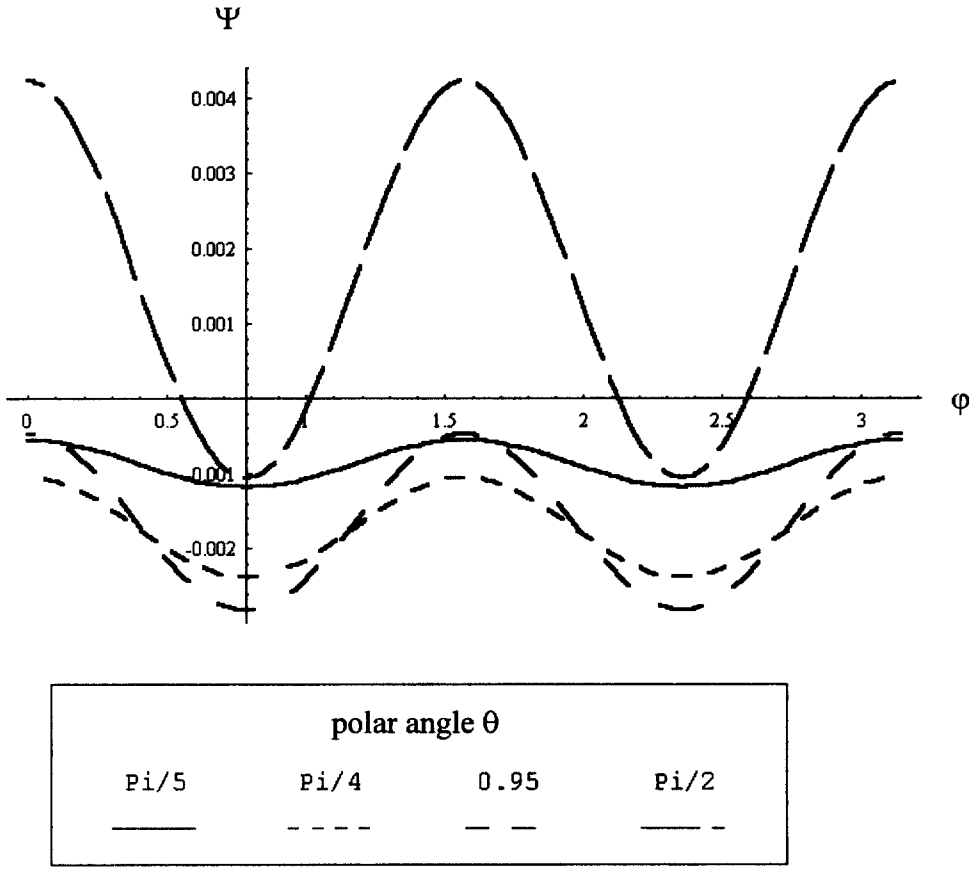

Fig. 8. On the location of the extremes of the energy $\psi(R_1, R_2, R_3)$: sectional cuts.

the "holes" around the center are an artifact due to the graphics software used. They characterize regions where the two spheres would interpenetrate each other, a case which is not covered in eqn (5.13).

Figure 7(b) shows $\psi(R_1, R_2 = R_\xi/\sqrt{3}, R_3)$ for the choice $\rho_1 = 1$, $\rho_2 = \frac{1}{5}$ which covers the behavior of the energy within a plane parallel to the plane (R_1, R_3) through the minimum $[R_\xi, \pi/4, \arccos(1/\sqrt{3})]$ (cf., Table 2). Due to symmetry this minimum occurs with a periodicity of $\pi/2$. Moreover the function goes through maxima at positions shifted by $\pi/2$ with respect to the minima. As in Fig. 7(a) the hole in the center is a graphical artifact.

The behavior of $\psi(R_1, R_2, R_3)$ is examined in more detail in Fig. 8 which shows sectional cuts at different angles of the 3-D graph of Fig. 7.

Summarizing one may say that if $\varepsilon_1^* \varepsilon_2^*$ is positive, in other words, if the eigenstrains of the inclusions are both expansive or both contractive in nature, a simple cubic arrangement of precipitates with respect to main crystallographic axes minimizes the elastic energy.† On the other hand, if ε_1^* and ε_2^* have alternating signs the energy is minimized when the inclusions are arranged in a body-centered or face-centered cubic structure.

6. CONCLUSIONS AND OUTLOOK

Continuous Fourier transforms (CFT) were used to derive closed-form expression for the total strains inside and outside of a dilatorically eigenstrained spherical inclusion in an infinite body, both made of the same cubic material with the same orientation of crystallographic axes. The solution is approximate with respect to the anisotropy coefficient. It was demonstrated by means of discrete Fourier transforms (DFT) that the overall behavior of the strains is still well represented by this solution, even for highly anisotropic

† This corresponds to the maxima of $\psi(R_1, R_2, R_3)$ (note that μ^* and, consequently, $\tilde{B}$ are negative!).

materials. However, the maximum of the strains is slightly underpredicted. Moreover, CFT was used for explicit computation of the total elastic energy due to the dilatoric misfit of two differently sized spheres in a cubic matrix. The expression was written as a function of relative distance of the two spheres as well as their orientation with respect to the main crystallographic axes. Moreover, it was examined for minima in order to explain the occurrence of preferred points of location during precipitation in anisotropic solids.

REFERENCES

Auld, B. A. (1990) *Acoustics Fields and Waves in Solids*, Vol. I, 2nd edn. Krieger, Malabar, Florida.

Dreyer, W. (1995) Development of microstructure based viscoplastic models for an advanced design of single crystal hot section components. In: *Periodic Progress Report, Development of Microstructural Based Viscoplastic Models for an Advanced Design of Single Crystal Hot Section Components*, ed. J. Olschewski. Brite/Euram Programme, A.1-17–A.1-29.

Dreyer, W. and Olschewski, J. (1994) Order–disorder transitions under load in single crystal superalloys: theory. In *Solid → Solid Phase Transformations*, ed. W. C. Johnson, J. M. Howe, D. E. Laughlin and W. A. Soffa, pp. 419–424. The Minerals, Metals and Materials Society.

Dreyer, W., Müller, W. H. and Olschewski, J. (1997) An approximate analytical 2-D solution for the stresses and strains in eigenstrained cubic materials. *Acta Mechanica*, submitted.

Gradshteyn, I. S. and Ryzhik, I. M. (1980) *Table of Integrals, Series, and Products*. Academic Press, New York.

Hazotte, A. and Lacaze, J. (1994) Caractérisation quantitative de la microstructure des superalliages à base de nickel. *La Revue de Métallurgie-CIT/Science et Génie des Matériaux*, Février 1994, pp. 277–294.

Ignat, M., Buffiere, J.-Y. and Chaix, J. M. (1993) Microstructures induced by a stress gradient in a nickel-base superalloy. *Acta metall. mater.* **41**(3), 855–862.

Khachaturyan, A. G. and Shatalov, G. A. (1969) Elastic-interaction potential of defects in a crystal. *Soviet Physics—Solid State* **11**(1), 118–123.

Mader, W. (1987) On the electron diffraction contrast caused by large inclusions. *Philosophical Magazine A* **55**(1), 59–83.

McCormack, M., Khachaturyan, A. G. and Morris, Jr, J. W. (1992) A two-dimensional analysis of the evolution of coherent precipitates in elastic media. *Acta Metall. Mater.* **40**(2), 325–336.

Mura, T. (1987) *Micromechanics of Defects in Solids*. Second revised edn. Martinus Nijhoff Publishers, Dordrecht, The Netherlands.

Moulinec, H. and Suquet, P. (1994) A fast numerical method for computing the linear and non-linear mechanical properties of composites. *C.R. Acad. Sci. Paris* **318**(II), 1417–1423.

Moulinec, H. and Suquet, P. (1996) A numerical method for computing the overall response of composites from images of their microstructures. In *Microstructure–Property Interactions in Composite Materials*, ed. R. Pyrz, pp. 235–246.

Moulinec, H. and Suquet, P. (1997) A numerical method for computing the overall response of nonlinear composites with complex microstructure. *Comp. Meth. Appl. Mech. Engng*, in print.

Müller, W. H. (1996) Mathematical vs experimental stress analysis of inhomogeneities in solids. *Journal de Physique IV. Colloque C1, supplément au Journal de Physique III* **6**, C1-139–C1-148.

Pineau, A. (1975) Influence of uniaxial stress on the morphology of coherent precipitates during coarsening—elastic energy considerations. *Acta Metallurgica* **24**, 559–564.

Socrate, S. and Parks, D. M. (1993) Numerical determination of the elastic driving force for directional coarsening in Ni-superalloys. *Acta metall. mater.* **41**(7), 2185–2209.

Tien, K. and Copley, S. M. (1970) The effect of orientation and sense of applied uniaxial stress on the morphology of coherent gamma prime precipitates in stress annealed nickel-base superalloy crystals. *Metallurgical Transactions* **2**, 543–553.

Wang, Y., Chen, L.-Q. and Khachaturyan, A. G. (1992) Particle translational motion and reverse coarsening phenomena in multiparticle systems induced by a long-range elastic interaction. *Physical Review B* **46**(17), 11,194–11,197.

Wolfram, S. (1992) *Mathematica® Ein System für Mathematik auf dem Computer*. Zweite Auflage. Addison-Wesley Publishing Company, Bonn.

APPENDIX A: PROOF OF EQNS (3.11)–(3.13)

For the proof of these equations it is necessary to know the Fourier transform of the step function, $\theta(\underline{x})$, for a spherical region of radius R. It is given by:

$$\hat{\theta}(k) = \frac{2}{\sqrt{2\pi}} \frac{1}{k^2} \left[\frac{\sin(kR)}{k} - R\cos(kR) \right] = \left(\frac{R}{k} \right)^{3/2} J_{3/2}(kR). \tag{A.1}$$

The latter becomes evident by means of eqn (8.463.1) from the book by Gradshteyn and Ryzhik (1980), and in order to prove the first equality the argument starts from the basic definition of a Fourier transform when applied to the step function:

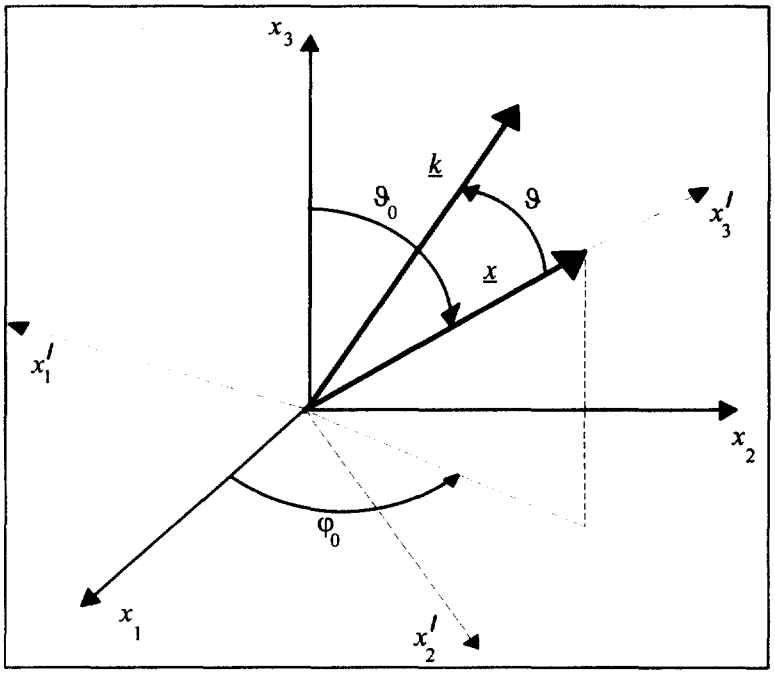

Fig. A.1. Orthogonal transformation of coordinates.

$$\hat{\theta}(\underline{k}) = \frac{1}{(2\pi)^{3/2}} \int_{-\infty}^{+\infty} \theta(\underline{x}) \exp(i\underline{k} \cdot \underline{x})\, \mathrm{d}\underline{x} = \frac{1}{(2\pi)^{3/2}} \int_0^R \mathrm{d}r r^2 \oint\!\!\int_{EK} \exp(i\underline{k} \cdot \underline{x}) \sin\vartheta\, \mathrm{d}\vartheta\, \mathrm{d}\varphi. \tag{A.2}$$

Now the coordinates are transformed as illustrated in Fig. A.1:

$$x'_m = O_{mi} x_i = (0, 0, r) \tag{A.3}$$

with an orthogonal matrix O_{ij}.

Consequently, the components of the position vector in Fourier space can be written as follows:

$$k'_m = O_{mi} k_i, \quad k'_m = (\cos\varphi \sin\vartheta, \sin\varphi \sin\vartheta, \cos\vartheta)k \tag{A.4}$$

and the following useful relations hold:

$$\underline{x} \cdot \underline{k} = x_i k_i = x_i O_{mi} k'_m = x'_m k'_m = r \cos\vartheta k. \tag{A.5}$$

Insertion of these eqns into eqn (A.2) results in:

$$\hat{\theta}(k) = \frac{1}{\sqrt{2\pi}} \int_0^R \mathrm{d}r r^2 \int_{-1}^{+1} \mathrm{d}\zeta \exp(ikr\zeta) = \frac{2}{\sqrt{2\pi}} \frac{1}{k} \int_0^R r \sin(kr)\, \mathrm{d}r \tag{A.6}$$

which can be integrated elementarily, q.e.d.

During the inverse transformation of the approximated eqns (3.8)–(3.10) for $\hat{\varepsilon}_{ij}$ use will be made of the same orthogonal transformation as in eqns (A.3) and (A.4) which reads explicitly:

$$O_{ij} = \begin{pmatrix} \cos\varphi_0 \cos\vartheta_0 & \sin\varphi_0 \cos\vartheta_0 & -\sin\vartheta_0 \\ -\sin\varphi_0 & \cos\varphi_0 & 0 \\ \cos\varphi_0 \sin\vartheta_0 & \sin\varphi_0 \sin\vartheta_0 & \cos\vartheta_0 \end{pmatrix}_{ij}. \tag{A.7}$$

After insertion of eqns (A.4), (A.5) and (A.7) into eqns (3.8)–(3.10) and using polar-coordinates the following equation for strain components is obtained when performing the inverse Fourier transform.†

$$\varepsilon_{ij}(\underline{x}) = E^{ij}_{lm} K_{rs} \delta_{lr} \delta_{ms} + E^{ij}_{lmno} K_{rstu} \delta_{lr} \delta_{ms} \delta_{nt} \delta_{ou} + E^{ij}_{lmnopq} K_{rstuvw} \delta_{lr} \delta_{ms} \delta_{nt} \delta_{ou} \delta_{pv} \delta_{qw}, \tag{A.8}$$

where the following symbols have been introduced:

† Einstein's summation rule applies unless the indices are underlined.

$$E^{ij}_{lm} = \frac{B\varepsilon_0}{(2\pi)^{3/2}}(1+\mu^*)O^{ij}_{lm}, \quad E^{ij}_{lmno} = -\frac{B\varepsilon_0}{(2\pi)^{3/2}}\mu^* O^{ijij}_{lmno}, \tag{A.9}$$

$$E^{ij}_{lmnopq} = -\frac{B\varepsilon_0}{(2\pi)^{3/2}}\mu^* B_1 O^{ij}_{lm} O^{\Sigma}_{nopq}, \tag{A.10}$$

$$E^{12}_{lm} = \frac{B\varepsilon_0}{(2\pi)^{3/2}}\left(1+\frac{\mu^*}{2}\right)O^{12}_{lm}, \quad E^{12}_{lmno} = \frac{B\varepsilon_0}{(2\pi)^{3/2}}\frac{\mu^*}{2}O^{1233}_{lmno}, \tag{A.11}$$

$$E^{12}_{lmnopq} = -\frac{B\varepsilon_0}{(2\pi)^{3/2}}\mu^* B_1 O^{lm}_{12} O^{nopq}_{\Sigma}, \tag{A.12}$$

$$K_{lm} = \int_{\mathscr{R}^3} \frac{k'_l k'_m}{k^2}\hat{\theta}(k)\exp(-irk\cos\vartheta)\,\mathrm{d}\underline{k}', \tag{A.13}$$

$$K_{lmno} = \int_{\mathscr{R}^3} \frac{k'_l k'_m k'_n k'_o}{k^4}\hat{\theta}(k)\exp(-irk\cos\vartheta)\,\mathrm{d}\underline{k}', \tag{A.14}$$

$$K_{lmnopq} = \int_{\mathscr{R}^3} \frac{k'_l k'_m k'_n k'_o k'_p k'_q}{k^6}\hat{\theta}(k)\exp(-irk\cos\vartheta)\,\mathrm{d}\underline{k}', \tag{A.15}$$

$$O^{ab}_{lm} = O_{la}O_{mb}, \quad O^{abcd}_{lmno} = O_{la}O_{mb}O_{nc}O_{od}, \quad \text{for } a,b,c,d = 1,2,3, \tag{A.16}$$

$$O^{nopq}_{\Sigma} = O_{n1}O_{o1}O_{p2}O_{q2} + O_{n1}O_{o1}O_{p3}O_{q3} + O_{n2}O_{o2}O_{p3}O_{q3}. \tag{A.17}$$

To perform the remaining integrations in eqns (A.13)–(A.15) polar coordinates will be used:

$$K_{rs} = \tilde{F}_{\underline{rs}}\bar{P}_{\underline{rs}}, \quad K_{rstu} = \tilde{F}_{\underline{rstu}}\bar{P}_{\underline{rstu}}, \quad K_{rstuvw} = \tilde{F}_{\underline{rstuvw}}\bar{P}_{\underline{rstuvw}}, \tag{A.18}$$

with the following factorized integrals:

$$\tilde{F}_{rs} = \int_0^{2\pi} F_{rs}(\varphi)\,\mathrm{d}\varphi, \quad \tilde{F}_{rstu} = \int_0^{2\pi} F_{rstu}(\varphi)\,\mathrm{d}\varphi, \quad \tilde{F}_{rstuvw} = \int_0^{2\pi} F_{rstuvw}(\varphi)\,\mathrm{d}\varphi, \tag{A.19}$$

$$\bar{P}_{rs} = \int_0^{\infty} k^2\hat{\theta}(k)\tilde{P}_{rs}(k)\,\mathrm{d}k, \quad \bar{P}_{rstu} = \int_0^{\infty} k^2\hat{\theta}(k)\tilde{P}_{rstu}(k)\,\mathrm{d}k, \quad \bar{P}_{rstuvw} = \int_0^{\infty} k^2\hat{\theta}(k)\tilde{P}_{rstuvw}(k)\,\mathrm{d}k, \tag{A.20}$$

$$\tilde{P}_{rs}(k) = \int_0^{\pi} P_{rs}(\vartheta)\sin\vartheta\exp(-irk\cos\vartheta)\,\mathrm{d}\vartheta, \quad \tilde{P}_{rstu}(k) = \int_0^{\pi} P_{rstu}(\vartheta)\sin\vartheta\exp(-irk\cos\vartheta)\,\mathrm{d}\vartheta,$$

$$\tilde{P}_{rstuvw}(k) = \int_0^{\pi} P_{rstuvw}(\vartheta)\sin\vartheta\exp(-irk\cos\vartheta)\,\mathrm{d}\vartheta, \tag{A.21}$$

and

$$F_{rs}(\varphi) = \cos^{\overset{2}{\delta}_1}\varphi\sin^{\overset{2}{\delta}_2}\varphi, \quad F_{rstu}(\varphi) = \cos^{\overset{4}{\delta}_1}\varphi\sin^{\overset{4}{\delta}_2}\varphi, \quad F_{rstuvw}(\varphi) = \cos^{\overset{6}{\delta}_1}\varphi\sin^{\overset{6}{\delta}_2}\varphi \tag{A.22}$$

$$P_{rs}(\vartheta) = \cos^{\overset{2}{\delta}_3}\vartheta\sin^{\overset{2}{\delta}_1+\overset{2}{\delta}_2}\vartheta, \quad P_{rstu}(\vartheta) = \cos^{\overset{4}{\delta}_3}\vartheta\sin^{\overset{4}{\delta}_1-\overset{4}{\delta}_2}\vartheta, \quad P_{rstuvw}(\vartheta) = \cos^{\overset{6}{\delta}_3}\vartheta\sin^{\overset{6}{\delta}_1-\overset{6}{\delta}_2}\vartheta \tag{A.23}$$

$$\overset{2}{\delta}_1 = \delta_{r1}+\delta_{s1}, \quad \overset{2}{\delta}_2 = \delta_{r2}+\delta_{s2}, \quad \overset{2}{\delta}_3 = \delta_{r3}+\delta_{s3}, \tag{A.24}$$

$$\overset{4}{\delta}_1 = \delta_{r1}+\delta_{s1}+\delta_{t1}+\delta_{u1}, \quad \delta_2 = \delta_{r2}+\delta_{s2}+\delta_{t2}+\delta_{u2}, \quad \overset{4}{\delta}_3 = \delta_{r3}+\delta_{s3}+\delta_{t3}+\delta_{u3}, \tag{A.25}$$

$$\overset{6}{\delta}_1 = \delta_{r1}+\delta_{s1}+\delta_{t1}+\delta_{u1}+\delta_{v1}+\delta_{w1}, \quad \delta_2 = \delta_{r2}+\delta_{s2}+\delta_{t2}+\delta_{u2}+\delta_{v2}+\delta_{w2},$$
$$\overset{6}{\delta}_3 = \delta_{r3}+\delta_{s3}+\delta_{t3}+\delta_{u3}+\delta_{v3}+\delta_{w3}. \tag{A.26}$$

It should be noted that F_{rs}, F_{rstu}, F_{rstuvw}, P_{rs}, P_{rstu}, P_{rstuvw} have the following symmetry properties:

$$F_{rs} = F_{sr}, \quad F_{rstu} = F_{rsut} = F_{rtsu} = F_{rtus} = \cdots, \quad \text{etc.},$$
$$P_{rs} = P_{sr}, \quad P_{rstu} = P_{rsut} = P_{rtsu} = P_{rtus} = \cdots, \quad \text{etc.} \tag{A.27}$$

Because of:

Table A.1. Results of the φ-integrations (the third row shows a representative, and the fourth row contains the general symbol)

Two indices		Four indices				Six indices					
w/o 3s	two 3s	w/o 3s	two 3s	four 3s		w/o 3s		two 3s		four 3s	six 3s
$\tilde{F}_{11}$	$\tilde{F}_{33}$	$\tilde{F}_{1111}$	$\tilde{F}_{1122}$	$\tilde{F}_{1133}$	$\tilde{F}_{3333}$	$\tilde{F}_{111111}$	$\tilde{F}_{111122}$	$\tilde{F}_{111133}$	$\tilde{F}_{112233}$	$\tilde{F}_{113333}$	$\tilde{F}_{333333}$
$\overset{2}{F}{}^{1}_{0}$	$\overset{2}{F}{}^{1}_{2}$	$\overset{4}{F}{}^{1}_{0}$	$\overset{4}{F}{}^{2}_{0}$	$\overset{4}{F}{}^{1}_{2}$	$\overset{4}{F}{}^{1}_{4}$	$\overset{6}{F}{}^{1}_{0}$	$\overset{6}{F}{}^{2}_{0}$	$\overset{6}{F}{}^{1}_{2}$	$\overset{6}{F}{}^{2}_{2}$	$\overset{6}{F}{}^{1}_{4}$	$\overset{6}{F}{}^{1}_{6}$
π	2π	$3\pi/4$	$\pi/4$	π	2π	$5\pi/8$	$\pi/8$	$3\pi/4$	$\pi/4$	π	2π

$$\begin{aligned}
\tilde{F}_{rs} &= 0, \quad \text{if } \overset{2}{\delta}_1 \text{ and } \overset{2}{\delta}_2 \text{ are odd,} \\
\tilde{F}_{rstu} &= 0, \quad \text{if } \overset{4}{\delta}_1 \text{ and } \overset{4}{\delta}_2 \text{ are odd,} \\
\tilde{F}_{rstuvw} &= 0, \quad \text{if } \overset{6}{\delta}_1 \text{ and } \overset{6}{\delta}_2 \text{ are odd,}
\end{aligned} \tag{A.28}$$

and:

$$\begin{aligned}
&\tilde{F}_{11} = \tilde{F}_{22}, \quad \tilde{F}_{1111} = \tilde{F}_{2222}, \quad \tilde{F}_{111111} = \tilde{F}_{222222}, \quad \tilde{F}_{112222} = \tilde{F}_{221111} \\
&\tilde{F}_{111133} = \tilde{F}_{222233}, \quad \tilde{F}_{113333} = \tilde{F}_{223333},
\end{aligned} \tag{A.29}$$

all components of F_{rs}, F_{rstu} and F_{rstuvw} can be reduced to twelve integrals which can easily be evaluated using eqns (2.511.1)–(2.511.4) from the monograph of Gradshteyn and Ryzhik (1980). The results are presented in Table A.1.

With regards to the angle ϑ nine integrals have to be solved. To this end formula (8.411) from Gradshteyn and Ryzhik (1980) can be used:

$$\begin{aligned}
&\int_0^\pi \sin\vartheta \exp(-\mathrm{i}rk\cos\vartheta)\,\mathrm{d}\vartheta = 2^{1/2}\Gamma(\tfrac{1}{2})(rk)^{-(1/2)}J_{1/2}(rk), \\
&\int_0^\pi \sin^3\vartheta \exp(-\mathrm{i}rk\cos\vartheta)\,\mathrm{d}\vartheta = 2^{3/2}\Gamma(\tfrac{1}{2})(rk)^{-(3/2)}J_{3/2}(rk), \\
&\int_0^\pi \sin^5\vartheta \exp(-\mathrm{i}rk\cos\vartheta)\,\mathrm{d}\vartheta = 2^{5/2}\Gamma(\tfrac{1}{2})\Gamma(3)(rk)^{-(5/2)}J_{5/2}(rk), \\
&\int_0^\pi \sin^7\vartheta \exp(-\mathrm{i}rk\cos\vartheta)\,\mathrm{d}\vartheta = 2^{7/2}\Gamma(\tfrac{1}{2})\Gamma(4)(rk)^{-(7/2)}J_{7/2}(rk).
\end{aligned} \tag{A.30}$$

Table A.2 contains the final results of the ϑ-integration. The remaining integration with respect to k can be accomplished by means of formulae (6.574.1) and (6.574.3) from Gradshteyn and Ryzhik (1980). Table A.3 presents the final results.

With the results of Tables A.1 and A.3 it is possible to successively evaluate the terms on the right hand side of eqn (A.8):

$$K_{rs}\delta_{lr}\delta_{ms} = \overset{2}{T}_0\delta_{lm} + \overset{2}{T}_2\delta_{l3}\delta_{m3} \tag{A.31}$$

with:

$$\overset{2}{T}_0 = \overset{2}{F}_0\overset{2}{\tilde{P}}_0, \quad \overset{2}{T}_2 = \overset{2}{F}_2\overset{2}{\tilde{P}}_2 - \overset{2}{F}_0\overset{2}{\tilde{P}}_0 \tag{A.32}$$

so that:

$$\begin{aligned}
&\text{in the inside:} \quad \overset{2}{T}_0 = (2\pi)^{3/2}\frac{1}{3}, \quad \overset{2}{T}_2 = 0, \\
&\text{in the outside:} \quad \overset{2}{T}_0 = (2\pi)^{3/2}\frac{1}{3}\frac{R^3}{r^3}, \quad \overset{2}{T}_2 = -(2\pi)^{3/2}\frac{R^3}{r^3}.
\end{aligned} \tag{A.33}$$

Similarly:

$$\begin{aligned}
K_{rstu}\delta_{lr}\delta_{ms}\delta_{nt}\delta_{ou} = {} & \overset{2}{T}_0(\delta_{lm}\delta_{no} + \delta_{ln}\delta_{mo} + \delta_{lo}\delta_{mn}) + \overset{4}{T}_2(\delta_{l3}\delta_{m3}\delta_{no} + \delta_{l3}\delta_{n3}\delta_{mo} + \delta_{l3}\delta_{o3}\delta_{mn} \\
& + \delta_{m3}\delta_{n3}\delta_{lo} + \delta_{m3}\delta_{o3}\delta_{ln} + \delta_{n3}\delta_{o3}\delta_{lm}) + \overset{4}{T}_4\delta_{l3}\delta_{m3}\delta_{n3}\delta_{o3}
\end{aligned} \tag{A.34}$$

with:

Table A.2. Results of the ϑ-integrations (the third row shows a representative, and the fourth row contains the general symbol)

Two indices		Four indices		
w/o 3s	two 3s	w/o 3s	two 3s	four 3s
$\tilde{P}_{11}(k)$	$\tilde{P}_{33}(k)$	$\tilde{P}_{1111}(k)$	$\tilde{P}_{1133}(k)$	$\tilde{P}_{3333}(k)$
$\overset{2}{P}_0(k) = 2^{3/2}\sqrt{\pi}(rk)^{-(3/2)}J_{3/2}(rk)$	$\overset{2}{P}_2(k) = 2^{1/2}\sqrt{\pi}(rk)^{-(1/2)}J_{1/2}(rk) - 2^{3/2}\sqrt{\pi}(rk)^{-(3/2)}J_{3/2}(rk)$	$\overset{4}{P}_0(k) = 2^{7/2}\sqrt{\pi}(rk)^{-(5/2)}J_{5/2}(rk)$	$\overset{4}{P}_2(k) = 2^{3/2}\sqrt{\pi}(rk)^{-(3/2)}J_{3/2}(rk) - 2^{7/2}\sqrt{\pi}(rk)^{-(5/2)}J_{5/2}(rk)$	$\overset{4}{P}_4(k) = 2^{1/2}\sqrt{\pi}(rk)^{-1/2}J_{1/2}(rk) - 2^{5/2}\sqrt{\pi}(rk)^{-(3/2)}J_{3/2}(rk) + 2^{7/2}\sqrt{\pi}(rk)^{-(5/2)}J_{5/2}(rk)$

Six indices			
w/o 3s	two 3s	four 3s	six 3s
$\tilde{P}_{111111}(k)$	$\tilde{P}_{111133}(k)$	$\tilde{P}_{113333}(k)$	$\tilde{P}_{333333}(k)$
$\overset{6}{P}_0(k) = 2^{7/2}6\sqrt{\pi}(rk)^{-(7/2)}J_{7/2}(rk)$	$\overset{6}{P}_2(k) = 2^{7/2}\sqrt{\pi}(rk)^{-(5/2)}J_{5/2}(rk) - 2^{7/2}6\sqrt{\pi}(rk)^{-(7/2)}J_{7/2}(rk)$	$\overset{6}{P}_4 = 2^{3/2}\sqrt{\pi}(rk)^{-(3/2)}J_{3/2}(rk) 2^{9/2}\sqrt{\pi}(rk)^{-(5/2)}J_{5/2}(rk) + 2^{7/2}6\sqrt{\pi}(rk)^{-(7/2)}J_{7/2}(rk)$	$\overset{6}{P}_6 = 2^{1/2}\sqrt{\pi}(rk)^{-(1/2)}J_{1/2}(rk) - 3\cdot 2^{3/2}\sqrt{\pi}(rk)^{-(3/2)}J_{3/2}(rk) + 3\cdot 2^{7/2}\sqrt{\pi}(rk)^{-(5/2)}J_{5/2}(rk) - 2^{7/2}6\sqrt{\pi}(rk)^{-(7/2)}J_{7/2}(rk)$

Table A.3. Results of the k-integrations†

Two indices

S	$\overset{2}{\bar{P}}_S$ inside the sphere	$\overset{2}{\bar{P}}_S$ outside the sphere
0	$\overset{2}{\bar{P}}_0 = \frac{2\sqrt{2\pi}}{3}$	$\overset{2}{\bar{P}}_0 = \frac{2\sqrt{2\pi}}{3}\frac{R^3}{r^3}$
2	$\overset{2}{\bar{P}}_2 = \overset{6}{\bar{P}}_2 = \frac{\sqrt{2\pi}}{3}$	$\overset{6}{\bar{P}}_2 = -\frac{2\sqrt{2\pi}}{3}\frac{R^3}{r^3}$

Four indices

S	$\overset{4}{\bar{P}}_S$ inside the sphere	$\overset{4}{\bar{P}}_S$ outside the sphere
0	$\overset{4}{\bar{P}}_0 = \overset{6}{\bar{P}}_0 = \frac{8\sqrt{2\pi}}{15}$	$\overset{4}{\bar{P}}_0 = \frac{4\sqrt{2\pi}R^3}{3r^3}\left(1-\frac{3}{5}\frac{R^2}{r^2}\right)$
2	$\overset{4}{\bar{P}}_2 = \overset{6}{\bar{P}}_2 = \frac{2\sqrt{2\pi}}{15}$	$\overset{4}{\bar{P}}_2 = \frac{2\sqrt{2\pi}R^3}{15r^3}\left(-5+6\frac{R^2}{r^2}\right)$
4	$\overset{4}{\bar{P}}_4 = \frac{\sqrt{2\pi}}{5}$	$\overset{4}{\bar{P}}_4 = -\frac{4\sqrt{2\pi}}{5}\frac{R^5}{r^5}$

Six indices

S	$\overset{6}{\bar{P}}_S$ inside the sphere	$\overset{6}{\bar{P}}_S$ outside the sphere
0	$\overset{6}{\bar{P}}_0 = \frac{16\sqrt{2\pi}}{35}$	$\overset{6}{\bar{P}}_0 = 2\sqrt{2\pi}\frac{R^3}{r^3}\left(1-\frac{6}{5}\frac{R^2}{r^2}+\frac{3}{7}\frac{R^4}{r^4}\right)$
2	$\overset{6}{\bar{P}}_2 = \frac{8\sqrt{2\pi}}{105}$	$\overset{6}{\bar{P}}_2 = \frac{2\sqrt{2\pi}R^3}{105r^3}\left(-35+84\frac{R^2}{r^2}-45\frac{R^4}{r^4}\right)$
4	$\overset{6}{\bar{P}}_4 = \frac{2\sqrt{2\pi}}{35}$	$\overset{6}{\bar{P}}_4 = \frac{2}{35}\sqrt{2\pi}\frac{R^3}{r^3}\left(-14\frac{R^2}{r^2}+15\frac{R^4}{r^4}\right)$
6	$\overset{6}{\bar{P}}_6 = \frac{\sqrt{2\pi}}{7}$	$\overset{6}{\bar{P}}_6 = -\frac{6\sqrt{2\pi}}{7}\frac{R^7}{r^7}$

† The meaning of the symbols becomes apparent by comparison with Table A.2.

$$\overset{4}{T}_0 = \overset{4}{F}_0^2\overset{4}{\bar{P}}_0, \quad \overset{4}{T}_2 = \overset{4}{F}_2^1\overset{4}{\bar{P}}_2 - \overset{4}{F}_0^2\overset{4}{\bar{P}}_0, \quad \overset{4}{T}_4 = \overset{4}{F}_4^1\overset{4}{\bar{P}}_4 - 6\overset{4}{F}_2^1\overset{4}{\bar{P}}_2 + 3\overset{4}{F}_0^2\overset{4}{\bar{P}}_0 \tag{A.35}$$

to be evaluated

in the inside:	in the outside:
$\overset{4}{T}_0 = \frac{(2\pi)^{3/2}}{15},$	$\overset{4}{T}_0 = (2\pi)^{3/2}\frac{1}{2}\frac{R^3}{r^3}\left(\frac{1}{3}-\frac{1}{5}\frac{R^2}{r^2}\right),$
$\overset{4}{T}_2 = 0,$	$\overset{4}{T}_2 = (2\pi)^{3/2}\frac{1}{2}\frac{R^3}{r^3}\left(-1+\frac{R^2}{r^2}\right),$
$\overset{4}{T}_4 = 0,$	$\overset{4}{T}_4 = (2\pi)^{3/2}\frac{1}{2}\frac{R^3}{r^3}\left(5-7\frac{R^2}{r^2}\right).$

(A.36)

And finally:

$$\begin{aligned}
K_{rstuvw}\delta_{lr}\delta_{ms}\delta_{nt}\delta_{ou}\delta_{pv}\delta_{qw} = {} & \overset{6}{T}_0(\delta_{lm}\delta_{no}\delta_{pq}+\delta_{lm}\delta_{np}\delta_{oq}+\delta_{lm}\delta_{nq}\delta_{op}+\delta_{ln}\delta_{mo}\delta_{pq}+\delta_{ln}\delta_{mp}\delta_{pq}+\delta_{ln}\delta_{mq}\delta_{op}\\
& +\delta_{lo}\delta_{nm}\delta_{pq}+\delta_{lo}\delta_{np}\delta_{mq}+\delta_{lo}\delta_{nq}\delta_{mp}+\delta_{lp}\delta_{mo}\delta_{nq}+\delta_{lp}\delta_{mn}\delta_{oq}+\delta_{lp}\delta_{mq}\delta_{on}+\delta_{lq}\delta_{mo}\delta_{np}+\delta_{lq}\delta_{mn}\delta_{op}+\delta_{lq}\delta_{mp}\delta_{on})\\
& +\overset{6}{T}_2([\delta_{no}\delta_{pq}+\delta_{np}\delta_{oq}+\delta_{nq}\delta_{op}]\delta_{l3}\delta_{m3}+[\delta_{mo}\delta_{pq}+\delta_{mp}\delta_{oq}+\delta_{mq}\delta_{op}]\delta_{l3}\delta_{n3}\\
& +[\delta_{mn}\delta_{pq}+\delta_{mp}\delta_{nq}+\delta_{mq}\delta_{np}]\delta_{l3}\delta_{o3}+[\delta_{mn}\delta_{oq}+\delta_{mo}\delta_{nq}+\delta_{mq}\delta_{no}]\delta_{l3}\delta_{p3}\\
& +[\delta_{mn}\delta_{po}+\delta_{mp}\delta_{no}+\delta_{mo}\delta_{np}]\delta_{l3}\delta_{q3}+[\delta_{ln}\delta_{pq}+\delta_{lp}\delta_{nq}+\delta_{lq}\delta_{np}]\delta_{m3}\delta_{o3}\\
& +[\delta_{lo}\delta_{pq}+\delta_{lp}\delta_{oq}+\delta_{lq}\delta_{op}]\delta_{m3}\delta_{n3}+[\delta_{ln}\delta_{po}+\delta_{lp}\delta_{no}+\delta_{lo}\delta_{np}]\delta_{m3}\delta_{q3}\\
& +[\delta_{lo}\delta_{nq}+\delta_{ln}\delta_{oq}+\delta_{lq}\delta_{on}]\delta_{m3}\delta_{p3}+[\delta_{lm}\delta_{po}+\delta_{lp}\delta_{mo}+\delta_{lo}\delta_{mp}]\delta_{n3}\delta_{q3}\\
& +[\delta_{lm}\delta_{pq}+\delta_{lp}\delta_{mq}+\delta_{lq}\delta_{mp}]\delta_{n3}\delta_{o3}+[\delta_{lm}\delta_{qo}+\delta_{lq}\delta_{mo}+\delta_{lo}\delta_{mq}]\delta_{n3}\delta_{p3}
\end{aligned}$$

$$+[\delta_{lm}\delta_{nq}+\delta_{ln}\delta_{mq}+\delta_{lq}\delta_{mn}]\delta_{o3}\delta_{p3}+[\delta_{lm}\delta_{np}+\delta_{ln}\delta_{mp}+\delta_{lp}\delta_{mn}]\delta_{o3}\delta_{q3}+[\delta_{lm}\delta_{no}+\delta_{ln}\delta_{mo}+\delta_{lo}\delta_{mn}]\delta_{p3}\delta_{q3})$$
$$+\overset{6}{T}_4([\delta_{o3}\delta_{pq}+\delta_{p3}\delta_{oq}+\delta_{q3}\delta_{op}]\delta_{l3}\delta_{m3}\delta_{n3}+[\delta_{p3}\delta_{nq}+\delta_{q3}\delta_{mp}]\delta_{l3}\delta_{m3}\delta_{o3}+\delta_{no}\delta_{l3}\delta_{m3}\delta_{p3}\delta_{q3}$$
$$+[\delta_{p3}\delta_{mq}+\delta_{q3}\delta_{mp}]\delta_{l3}\delta_{n3}\delta_{o3}+\delta_{mo}\delta_{l3}\delta_{n3}\delta_{p3}\delta_{q3}+\delta_{mn}\delta_{l3}\delta_{o3}\delta_{p3}\delta_{q3}$$
$$+[\delta_{p3}\delta_{lq}+\delta_{q3}\delta_{lp}]\delta_{m3}\delta_{n3}\delta_{o3}+\delta_{lo}\delta_{m3}\delta_{n3}\delta_{p3}\delta_{q3}+\delta_{ln}\delta_{m3}\delta_{o3}\delta_{q3}+\delta_{lm}\delta_{n3}\delta_{o3}\delta_{p3}\delta_{q3})+\overset{6}{T}_6\delta_{l3}\delta_{m3}\delta_{n3}\delta_{o3}\delta_{p3}\delta_{q3}, \tag{A.37}$$

where

$$\begin{aligned}
\overset{6}{T}_0 &= \tfrac{1}{15}\overset{6}{P}_0\overset{6}{F}{}^1_0,\\
\overset{6}{T}_2 &= \overset{6}{P}_2\overset{6}{F}{}^2_2-\tfrac{1}{15}\overset{6}{P}_0\overset{6}{F}{}^1_0,\\
\overset{6}{T}_4 &= \overset{6}{P}_4\overset{6}{F}{}^1_4-6\overset{6}{P}_2\overset{6}{F}{}^2_2+\tfrac{1}{5}\overset{6}{P}_0\overset{6}{F}{}^1_0,\\
\overset{6}{T}_6 &= \overset{6}{P}_6\overset{6}{F}{}^1_6-15\overset{6}{P}_4\overset{6}{F}{}^1_4+45\overset{6}{P}_2\overset{6}{F}{}^2_2-\overset{6}{P}_0\overset{6}{F}{}^1_0
\end{aligned} \tag{A.38}$$

to be evaluated as follows:

	in the inside:	in the outside:
$\overset{6}{T}_0$	$=\dfrac{(2\pi)^{3/2}}{105}$,	$\overset{6}{T}_0=(2\pi)^{3/2}\dfrac{1}{8}\dfrac{R^3}{r^3}\left(\dfrac{1}{3}-\dfrac{2}{5}\dfrac{R^2}{r^2}+\dfrac{1}{7}\dfrac{R^4}{r^4}\right)$,
$\overset{6}{T}_2$	$=0$,	$\overset{6}{T}_2=(2\pi)^{3/2}\dfrac{1R^3}{8r^3}\left(-1+2\dfrac{R^2}{r^2}-\dfrac{R^4}{r^4}\right)$,
$\overset{6}{T}_4$	$=0$,	$\overset{6}{T}_4=\dfrac{1}{2\pi\sqrt{2\pi}}\dfrac{1R^3}{8r^3}\left(5-14\dfrac{R^2}{r^2}+9\dfrac{R^4}{r^4}\right)$,
$\overset{6}{T}_6$	$=0$,	$\overset{6}{T}_6=\dfrac{1}{2\pi\sqrt{2\pi}}\dfrac{1R^3}{8r^3}\left(-35+126\dfrac{R^2}{r^2}-99\dfrac{R^4}{r^4}\right)$.

(A.39)

Insertion of these relations into eqn (A.8) for the strains completes the proof.

APPENDIX B: ELASTIC ENERGY OF TWO EIGENSTRAINED SPHERES

Similarly as in Section 3 the first step toward the calculation of the elastic energy shown in eqn (5.10) is to expand the denominator in $\hat{A}_{ijmn}$ from eqn (5.11) with respect to the parameter Λ and to neglect all non-linear terms in μ^*:

$$\Psi_{el}\approx\tilde{B}B_3\int_{\underline{k}}\left(2-B\mu^*\frac{k_\Sigma}{k^4}\right)\hat{\varepsilon}^*\overline{\hat{\varepsilon}^*}\,\mathrm{d}\underline{k} \tag{B.1}$$

where:

$$\tilde{B}=\frac{3\lambda+2\mu+\mu'}{2},\quad B=\frac{3\lambda+2\mu+\mu'}{\lambda+2\mu+\mu'},\quad B_3=\frac{2\mu+\mu'}{\lambda+2\mu+\mu'}. \tag{B.2}$$

Now the Fourier transform for the eigenstrains must be inserted. It can easily be obtained from eqns (5.1), (5.2) and (A.1):

$$\hat{\varepsilon}^*(\underline{k})=\hat{\theta}(\underline{k})\varepsilon_1^*+\hat{\theta}_2^R(\underline{k})\varepsilon_2^* \tag{B.3}$$

where:

$$\hat{\theta}_1(\underline{k})=\left(\frac{\rho_1}{k}\right)^{3/2}J_{3/2}(\rho_1 k),\quad \hat{\theta}_2^R(\underline{k})=\left(\frac{\rho_2}{k}\right)^{3/2}J_{3/2}(\rho_2 k)\exp(\mathrm{i}\underline{k}\cdot\underline{R}). \tag{B.4}$$

Consequently, it follows that:

$$\overline{(\varepsilon_1^*\hat{\theta}_1+\varepsilon_2^*\hat{\theta}_2^R)(\varepsilon_1^*\hat{\theta}_1+\varepsilon_2^*\hat{\theta}_2^R)} = \varepsilon_1^{*2}\hat{\theta}_1^2+2\varepsilon_1^*\varepsilon_2^*\hat{\theta}_1\ Re(\hat{\theta}_2)+\varepsilon_2^{*2}\hat{\theta}_2\theta_2^{*2}$$

$$= \varepsilon_1^{*2}\left(\frac{\rho_1}{k}\right)^{3/2} J_{3/2}(\rho_1 k)J_{3/2}(\rho_1 k)+2\varepsilon_1^*\varepsilon_2^*\frac{(\rho_1\rho_2)^{3/2}}{k^3}J_{3/2}(\rho_1 k)J_{3/2}(\rho_2 k)$$

$$+\varepsilon_2^{*2}\left(\frac{R_2}{k}\right)^{3/2} J_{3/2}(\rho_2 k)J_{3/2}(\rho_2 k)\cos(\underline{R}\cdot\underline{k}). \tag{B.5}$$

In order to solve the remaining integrals it is advantageous to perform an orthogonal transformation analogously to the one of Appendix A where the position $\underline{x}$ is replaced by the distance vector $\underline{R}$. Therefore:

$$\Psi_{el} = \Psi^1+\Psi^2, \tag{B.6}$$

with:

$$\Psi^1 = 2\tilde{B}B_3\int_{\mathcal{R}^3}\Psi(\underline{k'})\,\mathrm{d}\underline{k'}, \tag{B.7}$$

$$\Psi^2 = E_{lmno}\int_{\mathcal{R}^3}\frac{k'_l k'_m k'_n k'_o}{k'^4}\Psi(\underline{k'})\,\mathrm{d}\underline{k'} \tag{B.8}$$

and:

$$E_{lmno} = -\tilde{B}BB_3\mu^*(O_{l1}O_{m1}O_{n2}O_{o2}+O_{l1}O_{m1}O_{n3}O_{o3}+O_{l2}O_{m2}O_{n3}O_{o3}). \tag{B.9}$$

Using polar coordinates these relations can be evaluated as follows:

$$\Psi^1 = 2\tilde{B}B_3(\varepsilon_1^{*2}\rho_1^3\Psi^{1,1}+\varepsilon_2^{*2}\rho_2^3\Psi^{1,2}+2\varepsilon_1^*\varepsilon_2^*(\rho_1\rho_2)^{3/2}\Psi^{1,3}), \tag{B.10}$$

where:

$$\Psi^{1,1} = \int_0^{2\pi}\mathrm{d}\varphi\int_0^\infty k^{-1}J_{3/2}(\rho_1 k)J_{3/2}(\rho_1 k)\,\mathrm{d}k\int_0^\pi\sin\vartheta\,\mathrm{d}\vartheta,$$

$$\Psi^{1,2} = \int_0^{2\pi}\mathrm{d}\varphi\int_0^\infty k^{-1}J_{3/2}(\rho_2 k)J_{3/2}(\rho_2 k)\,\mathrm{d}k\int_0^\pi\sin\vartheta\,\mathrm{d}\vartheta,$$

$$\Psi^{1,3} = \int_0^{2\pi}\mathrm{d}\varphi\int_0^\infty k^{-1}J_{3/2}(\rho_1 k)J_{3/2}(\rho_2 k)\,\mathrm{d}k\int_0^\pi\cos(Rk\cos\vartheta)\sin\vartheta\,\mathrm{d}\vartheta\,\mathrm{d}k, \tag{B.11}$$

and:

$$\Psi^2 = E_{lmno}(\varepsilon_1^{*2}\rho_1^3\tilde{F}_{rstu}\tilde{\tilde{P}}^1_{rstu}+\varepsilon_2^{*2}\rho_2^3\tilde{F}_{rstu}\tilde{\tilde{P}}^2_{rstu}+2\varepsilon_1^*\varepsilon_2^*(\rho_1\rho_2)^{3/2}\tilde{F}_{rstu}\tilde{\tilde{P}}^3_{rstu})\delta_{rn}\delta_{so}\delta_{tp}\delta_{uq}, \tag{B.12}$$

with:

$$F_{rstu}(\varphi) = \cos^{\overset{4}{\delta}_1}\varphi\sin^{\overset{4}{\delta}_2}\varphi,\quad \tilde{F}_{rstu} = \int_0^{2\pi}F_{rstu}(\varphi)\,\mathrm{d}\varphi,\quad P_{rstu}(\vartheta) = \sin^{\overset{4}{\delta}_1+\overset{4}{\delta}_2}\vartheta\cos^{\overset{4}{\delta}_3}\vartheta,$$

$$\tilde{P}^1_{rstu} = \int_0^\pi P_{rstu}(\vartheta)\sin\vartheta\,\mathrm{d}\vartheta,\quad \tilde{P}^3_{rstu}(k) = \int_0^\pi P_{rstu}(\vartheta)\sin\vartheta\cos(Rk\cos\vartheta)\,\mathrm{d}\vartheta,$$

$$\tilde{\tilde{P}}^1_{rstu} = \tilde{P}^1_{rstu}\int_0^\infty k^{-1}J_{3/2}(\rho_1 k)J_{3/2}(\rho_1 k)\,\mathrm{d}k,\quad \tilde{\tilde{P}}^2_{rstu} = \tilde{P}^1_{rstu}\int_0^\infty k^{-1}J_{3/2}(\rho_2 k)J_{3/2}(\rho_2 k)\,\mathrm{d}k,$$

$$\tilde{\tilde{P}}^3_{rstu} = \int_0^\infty k^{-1}\tilde{P}^3_{rstu}(k)J_{3/2}(\rho_1 k)J_{3/2}(\rho_2 k)\,\mathrm{d}k. \tag{B.13}$$

The symbols $\overset{4}{\delta}_1$, $\overset{4}{\delta}_2$ and $\overset{4}{\delta}_3$ have been defined in eqns (A.24)–(A.26) of Appendix A.

Now the first part of the energy, Ψ^1, can be determined by means of eqns (6.574.2) and (6.573) from the book of Gradshteyn and Ryzhik (1980):

Table B.1. Results of the φ-integrations

Four indices				
Number of 3s in the indices	0		2	4
Representative of the component	$\tilde{F}_{1111}, \tilde{F}_{2222}$	$\tilde{F}_{1122}$	$\tilde{F}_{1133}$	$\tilde{F}_{3333}$
Integrand	$\sin^4\varphi, \cos^4\varphi$	$\sin^2\varphi\cos^2\varphi$	$\sin^2\varphi$	1
Value of the integral	$\overset{4}{F}{}_0^1 = 3\pi/4$	$\overset{4}{F}{}_0^2 = \pi/4$	$\overset{4}{F}{}_2^1 = \pi$	$\overset{4}{F}{}_4^1 = 2\pi$

$$\Psi^1 = \tfrac{8}{3}\pi\tilde{B}B_3(\varepsilon_1^{*2}\rho_1^3 + \varepsilon_2^{*2}\rho_2^3). \tag{B.14}$$

The second part of the energy can be computed analogously as outlined before. It should be noted that the symmetry conditions (A.27) hold so that the φ-integration is identical to the one of Appendix A. Consequently: and:

$$\Psi^2 = T_0(E_{llnn} + E_{lmlm} + E_{lnnl}) + T_2(E_{33nn} + E_{3m3m} + E_{3mm3} + E_{l33l} + E_{l3l3} + E_{ll33}) + T_4 E_{3333} \tag{B.15}$$

with:

$$\begin{aligned}
T_0 &= \frac{\pi}{4}(\varepsilon_1^{*2}\rho_1^3\tilde{\tilde{P}}^{1,0} + \varepsilon_2^{*2}\rho_2^3\tilde{\tilde{P}}^{2,0} + 2\varepsilon_1^*\varepsilon_2^*(\rho_1\rho_2)^{3/2}\tilde{\tilde{P}}^{3,0}),\\
T_2 &= \pi(\varepsilon_1^{*2}\rho_1^3\tilde{\tilde{P}}^{1,2} + \varepsilon_2^{*2}\rho_2^3\tilde{\tilde{P}}^{2,2} + 2\varepsilon_1^*\varepsilon_2^*(\rho_1\rho_2)^{3/2}\tilde{\tilde{P}}^{3,2})\\
&\quad - \frac{\pi}{4}(\varepsilon_1^{*2}\rho_1^3\tilde{\tilde{P}}^{1,0} + \varepsilon_2^{*2}\rho_2^3\tilde{\tilde{P}}^{2,0} + 2\varepsilon_1^*\varepsilon_2^*(\rho_1\rho_2)^{3/2}\tilde{\tilde{P}}^{3,0}),\\
T_4 &= 2\pi(\varepsilon_1^{*2}\rho_1^3\tilde{\tilde{P}}^{1,4} + \varepsilon_2^{*2}\rho_2^3\tilde{\tilde{P}}^{2,4} + 2\varepsilon_1^*\varepsilon_2^*(\rho_1\rho_2)^{3/2}\tilde{\tilde{P}}^{3,4})\\
&\quad - 6\pi(\varepsilon_1^{*2}\rho_1^3\tilde{\tilde{P}}^{1,2} + \varepsilon_2^{*2}\rho_2^3\tilde{\tilde{P}}^{2,2} + 2\varepsilon_1^*\varepsilon_2^*(\rho_1\rho_2)^{3/2}\tilde{\tilde{P}}^{3,2})\\
&\quad + \frac{3\pi}{4}(\varepsilon_1^{*2}\rho_1^3\tilde{\tilde{P}}^{1,0} + \varepsilon_2^{*2}\rho_2^3\tilde{\tilde{P}}^{2,0} + 2\varepsilon_1^*\varepsilon_2^*(\rho_1\rho_2)^{3/2}\tilde{\tilde{P}}^{3,0}).
\end{aligned} \tag{B.16}$$

In these eqns $\tilde{\tilde{P}}^{1,0}, \tilde{\tilde{P}}^{1,2}, \ldots$ are determined by the numbers of threes appearing in the indices and, therefore, only six ϑ- and five k-integrations remain. The ϑ-integration will be performed by means of eqns (2.511) and (8.411.5) from Gradshteyn and Ryzhik (1980):

In order to solve the k-integrals eqn (6.574.2) from Gradshteyn and Ryzhik (1980) can be applied:

$$\tilde{\tilde{P}}^{1,0} = \tilde{\tilde{P}}^{2,0} = \tfrac{16}{45}, \quad \tilde{\tilde{P}}^{1,2} = \tilde{\tilde{P}}^{2,2} = \tfrac{4}{45}, \quad \tilde{\tilde{P}}^{1,4} = \tilde{\tilde{P}}^{2,4} = \tfrac{2}{15}. \tag{B.17}$$

The evaluation of $\tilde{\tilde{P}}^{3,0}$, $\tilde{\tilde{P}}^{3,2}$ and $\tilde{\tilde{P}}^{3,4}$ becomes possible with the help of eqns (6.573.1), (6.573.2) and (6.578.1) from the same source. For the case that the two spheres do not interpenetrate the quantities $\tilde{\tilde{P}}^{3,0}$, $\tilde{\tilde{P}}^{3,2}$ and $\tilde{\tilde{P}}^{3,4}$ are given by:

$$\begin{aligned}
\tilde{\tilde{P}}^{3,0} &= \frac{8}{9}\frac{(\rho_1\rho_2)^{3/2}}{R^3}\left(1 - \frac{3}{5}\frac{R_1^2 + R_2^2}{R^2}\right),\\
\tilde{\tilde{P}}^{3,2} &= \frac{4}{9}\frac{(\rho_1\rho_2)^{3/2}}{R^3}\left(-1 + \frac{6}{5}\frac{R_1^2 + R_2^2}{R^2}\right),\\
\tilde{\tilde{P}}^{3,4} &= -\frac{8}{15}\frac{(\rho_1\rho_2)^{3/2}}{R^3}\frac{R_1^2 + R_2^2}{R^2}.
\end{aligned} \tag{B.18}$$

Hence it follows that T_0, T_2 and T_4 are given by:

Table B.2. Results of the ϑ-integrations

Number of 3s in the indices		
0	2	4
Representative of the component		
$\tilde{P}^1_{1111}$	$\tilde{P}^1_{1133}, \tilde{P}^1_{2323}$	$\tilde{P}^1_{3333}$
Integral to solve		
$\int_0^\pi \sin^5\vartheta\,\mathrm{d}\vartheta$	$\int_0^\pi \sin^3\vartheta\cos^2\vartheta\,\mathrm{d}\vartheta$	$\int_0^\pi \sin\vartheta\cos^4\vartheta\,\mathrm{d}\vartheta$
Value of the integral		
$\tilde{P}^{1,0} = \tilde{P}^{2,0} = \frac{16}{15}$	$\tilde{P}^{1,2} = \tilde{P}^{2,2} = \frac{4}{15}$	$\tilde{P}^{1,4} = \tilde{P}^{2,4} = \frac{2}{5}$
Representative of the component		
$\tilde{P}^3_{1111}$	$\tilde{P}^3_{1133}$	$\tilde{P}^3_{3333}$
Integral to solve		
$\int_0^\pi \sin^5\vartheta \times \cos(Rk\cos\vartheta)\,\mathrm{d}\vartheta$	$\int_0^\pi \sin^3\vartheta \times \cos^2\vartheta\cos(Rk\cos\vartheta)\,\mathrm{d}\vartheta$	$\int_0^\pi \sin\vartheta\cos^4\vartheta \times \cos(Rk\cos\vartheta)\,\mathrm{d}\vartheta$
Value of the integral		
$\tilde{P}^{3,0}(k) =$	$\tilde{P}^{3,2}(k) =$	$\tilde{P}^{3,4}(k) =$
$2^{1/2}\Gamma(\frac{1}{2})R^{-(1/2)}k^{-(1/2)}J_{1/2}(Rk)$	$2^{1/2}\Gamma(\frac{1}{2})R^{-(3/2)}k^{-(3/2)}J_{3/2}(Rk)$	$2^{1/2}\Gamma(\frac{1}{2})R^{-(1/2)}k^{-(1/2)}J_{1/2}(Rk)$
	$-2^{3/2}\Gamma(\frac{1}{2})R^{-(3/2)}k^{-(3/2)}J_{3/2}(Rk)$	$-2^{5/2}\Gamma(\frac{1}{2})R^{-(3/2)}k^{-(3/2)}J_{3/2}(Rk)$
		$+2^{7/2}\Gamma(\frac{1}{2})R^{-(5/2)}k^{-(5/2)}J_{5/2}(Rk)$

$$T_0 = \frac{4\pi}{45}\left((\varepsilon_1^{*2}\rho_1^3 + \varepsilon_2^{*2}\rho_2^3) + \varepsilon_1^*\varepsilon_2^*\frac{(\rho_1\rho_2)^3}{R^3}\left(5 - 3\frac{R_1^2+R_2^2}{R^2}\right)\right),$$

$$T_2 = \frac{4\pi}{3}\varepsilon_1^*\varepsilon_2^*\frac{(\rho_1\rho_2)^3}{R^3}\left(-1 + \frac{R_1^2+R_2^2}{R^2}\right),$$

$$T_4 = \frac{4\pi}{3}\varepsilon_1^*\varepsilon_2^*\frac{(\rho_1\rho_2)^3}{R^3}\left(5 - 7\frac{R_1^2+R_2^2}{R^2}\right). \tag{B.19}$$

Taking into account, that:

$$E_{llmm} = -3\tilde{B}BB_3\mu^*, \quad E_{lmml} = E_{lmlm} = 0,$$

$$E_{33nn} = -\tilde{B}BB_3\mu^*\frac{2R_1^2+R_2^2}{R^2}, \quad E_{ll33} = -\tilde{B}BB_3\mu^*\frac{R_2^2+2R_3^2}{R^2}$$

$$E_{3333} = -\tilde{B}BB_3\mu^*\frac{R_1^2R_2^2+R_1^2R_3^2+R_2^2R_3^2}{R^4}, \tag{B.20}$$

and that all other components of E_{lmno} vanish, concludes the proof.